



Synthesis and SAR of 4-aminocyclopentapyrrolidines as N-type Ca^{2+} channel blockers with analgesic activity

Xenia Beebe*, Daria Darczak, Rodger F. Henry, Timothy Vortherms, Richard Janis, Marian Namovic, Diana Donnelly-Roberts, Karen L. Kage, Carol Surowy, Ivan Milicic, Wende Niforatos, Andrew Swensen, Kennan C. Marsh, Jill M. Wetter, Pamela Franklin, Scott Baker, Chengmin Zhong, Gricelda Simler, Erica Gomez, Janel M. Boyce-Rustay, Chang Z. Zhu, Andrew O. Stewart, Michael F. Jarvis, Victoria E. Scott

Neuroscience Research, Global Pharmaceutical Research and Development, Abbott Laboratories, 100 Abbott Park Road, Abbott Park, IL 60064-6100, United States

ARTICLE INFO

Article history:

Received 14 March 2012

Revised 20 April 2012

Accepted 27 April 2012

Available online 4 May 2012

Keywords:

N-type calcium channel

L-type calcium channel

Analgesic activity

SAR

N-tert-Butyl sulfonamide

Enantioselective synthesis

ABSTRACT

A novel 4-aminocyclopentapyrrolidine series of N-type Ca^{2+} channel blockers have been discovered. Enantioselective synthesis of the 4-aminocyclopentapyrrolidines was enabled using *N*-tert-butyl sulfinamide chemistry. SAR studies demonstrate selectivity over L-type Ca^{2+} channels. N-type Ca^{2+} channel blockade was confirmed using electrophysiological recording techniques. Compound **25** is an N-type Ca^{2+} channel blocker that produces antinociception in inflammatory and nociceptive pain models without exhibiting cardiovascular or motor liabilities.

© 2012 Elsevier Ltd. All rights reserved.

1. Introduction

Voltage gated Ca^{2+} channels (VGCC) are involved in numerous neuronal functions including regulation of membrane ion conductance, neurotransmitter release, and cellular excitability. VGCCs control Ca^{2+} ion flow in and out of the cell in response to changes in membrane potential. The VGCC family includes both low voltage activated T-type (Cav3.1–3.3) Ca^{2+} channels and high voltage activated L-type (Cav1.1–1.4), N-type (Cav2.2), P/Q-type (Cav2.1) and R-type (Cav2.3) Ca^{2+} channels.^{1,2} Ten distinct mammalian genes encode the pore forming α_1 subunit of the Ca^{2+} channel.³ L-type Ca^{2+} channels are widely distributed in skeletal, cardiac, and smooth muscle tissue and are responsible for attenuating cardiovascular responses.⁴ The N-type and P/Q-type Ca^{2+} channels are located at presynaptic nerve terminals. N-type Ca^{2+} channels are responsible for the release of the neurotransmitters glutamate, substance P, and calcitonin gene-related peptide (CGRP) involved in pain signaling.^{5,6} The peptide ω -conotoxin GVIA is a potent and selective blocker of N-type Ca^{2+} channels and its derivative ziconotide (Prialt™) is used for the treatment of severe, chronic pain following intrathecal administration.⁷ Ziconotide is effective in patients that do not respond to other pain therapies and does

not cause tolerance, but it exhibits CNS side-effects such as sedation and hypotension.^{7,8} Small molecule N-type Ca^{2+} channel inhibitors that maintain analgesic efficacy with an improved therapeutic window compared to Prialt™ are an attractive pursuit for the treatment of chronic pain.

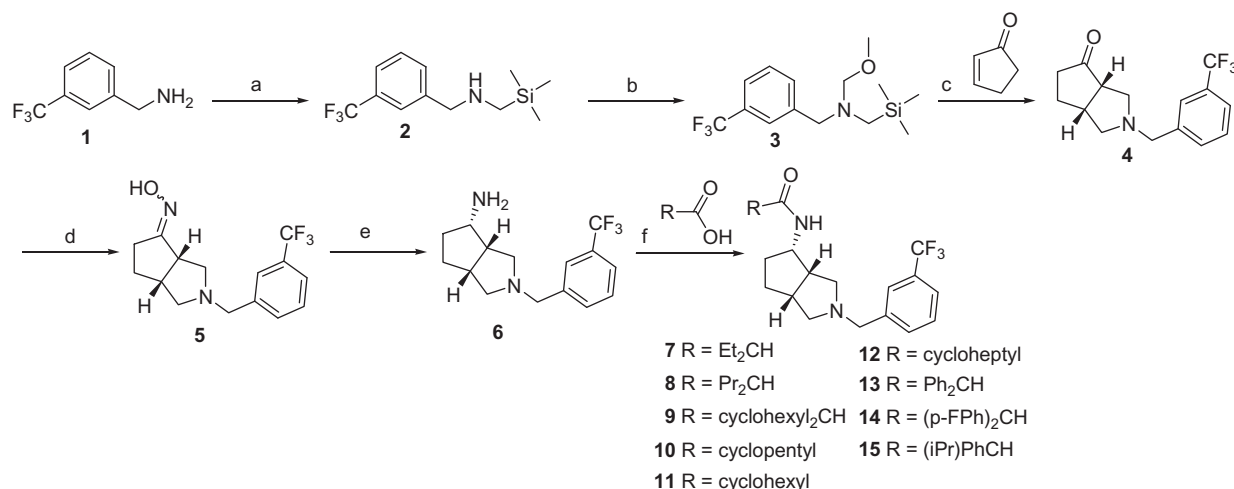
Research in the area of small molecule N-type Ca^{2+} channels inhibitors has been progressing in the last few years. Selectivity of N-type over L-type Ca^{2+} channels is key to discovering compounds with reduced cardiovascular liabilities.^{9–18} Additionally, identification of compounds that block the channel in a state-dependent manner (i.e., bind to the inactivated state of the channel more potently than the resting/closed state) may also enhance the therapeutic margins relative to Prialt™¹⁷ which lacks state-dependence. Herein we describe the discovery of a novel series of small molecule N-type Ca^{2+} blockers identified from screening the Abbott compound collection. The compounds were designed for N-type Ca^{2+} channel inhibition with selectivity over L-type Ca^{2+} channels with analgesic activity at doses that do not cause significant cardiovascular or motor coordination side-effects in animal models.

2. Chemistry

The synthesis of the 4-aminocyclopentapyrrolidines is outlined in Scheme 1. The core ketone **4** was constructed using a 1,3-dipolar cycloaddition via an azomethine ylid precursor **3**. The desired

* Corresponding author. Tel.: +1 847 937 8291; fax: +1 847 937 9195.

E-mail address: xenia.b.searle@abbott.com (X. Beebe).



Scheme 1. Reagents and conditions: (a) ClCH₂Si(CH₃)₃, Et₃N, 90 °C 16 h; (b) H₂CO, MeOH, K₂CO₃, 0 °C, 3 h; (c) TFA, CH₂Cl₂, rt, 45 min; (d) H₂NOH-HCl, NaOAc, H₂O/EtOH, 70 °C, 1 h; (e) H₂, Ra[®]-Ni, 20% NH₃/MeOH, rt, 16 h; (f) EDC, HOBT, CH₂Cl₂, rt, 16 h.

m-trifluoromethylbenzyl group was installed at the onset by combining *m*-trifluoromethylbenzylamine **1** with chloromethyltrimethylsilane to give amine **2** followed by reaction with formaldehyde and methanol to provide the azomethine ylid precursor **3**.¹⁹ Acid catalyzed azomethine ylid cyclization with cyclopenten-2-one proceeded smoothly to give the desired ketone **4** with syn stereochemistry at the ring juncture.^{20,21} Subsequent condensation with hydroxylamine gave a mixture of *E,Z* isomers of the oxime **5**. Reduction of the oxime **5** with Raney[®]-nickel catalyzed hydrogenation provided the amine **6** with all *cis* stereochemistry as the major product. Coupling of the amine with the appropriate acid provided amides **7–15**.

Enantiomeric resolution was performed as shown in Scheme 2 by condensing the ketone **16** with (*R*)-*tert*-butanesulfinamide **17** using titanium tetraethoxide.^{22,23} The resulting diastereomers were separated using silica gel chromatography with the *R,R,S*-diastereomer **18** eluting first and the *R,S,R*-diastereomer **19** eluting second.

Reduction of the *R,R,S*-diastereomer sulfinamide **18** with sodium borohydride at low temperature gave the all *cis* stereochemistry of the sulfinamide **20** as shown in Scheme 3. The absolute stereochemistry of the reduction product was determined by single crystal X-ray crystallography on compound **20** as shown in Figure 1.

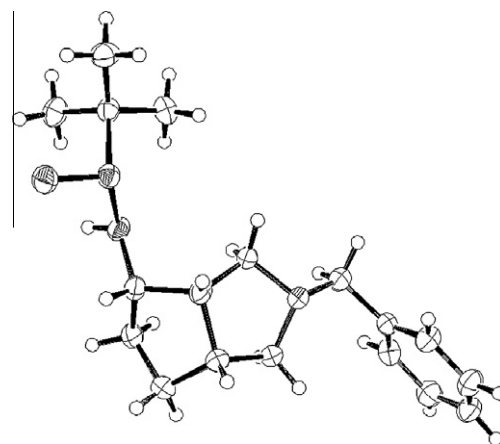


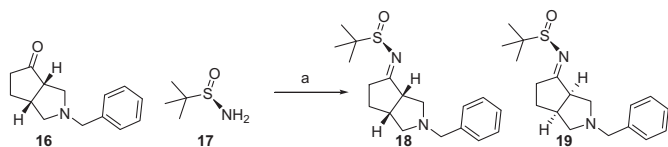
Figure 1. Ortep drawing of the X-ray crystal structure of sulfinamide **20**.

The stereochemistry of the hydride addition in this case is controlled by the cup-shaped bicyclic structure of the core and not by the chirality of the sulfinamide used. Other reducing agents such as *L*-selectride were used in an attempt to control the stereochemistry with the chiral auxiliary but only the all *cis* stereochemical product was obtained. When the opposite enantiomer (*S*)-*tert*-butanesulfinamide was used, the stereochemical outcome of the reduction was the same. Deprotection of the sulfinamide with acid gave the desired enantiomerically pure primary amine **21**.

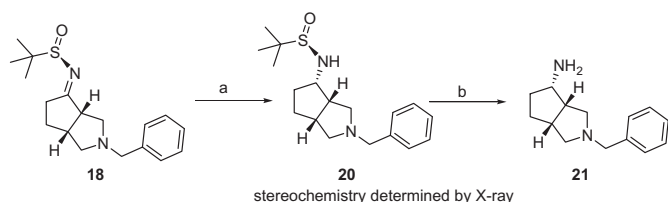
Synthesis of a single enantiomer of compound **25** and diversifying the *N*-benzyl group was accomplished as shown in Scheme 4. The enantiomerically pure amine was coupled with 2,2-dicyclohexylacetic acid **22** to give 2,2-dicyclohexylacetamide **23**. Subsequent debenzylation using Degussa catalyst provided pyrrolidine **24**. Reductive alkylation with the appropriate aldehyde using polymer-supported cyanoborohydride provided enantiomerically pure benzyl substituted compounds **25–31**.

The enantiomer of compound **25** was synthesized as shown in Scheme 5 and Scheme 6 starting with (*S*)-*tert*-butanesulfinamide provides the condensed products with the reversed order of elution; the *S,R,S*-diastereomer **33** eluting first followed by the *S,S,R*-diastereomer **34**.

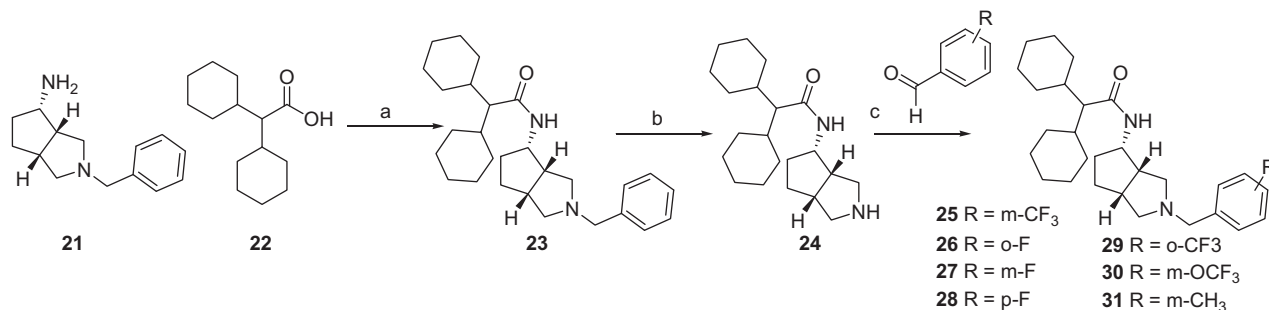
The desired isomer **33** was then reduced with sodium borohydride at low temperature in methanol to give **35** and the sulfinamide group deprotected to give the amine **36** with all *cis*



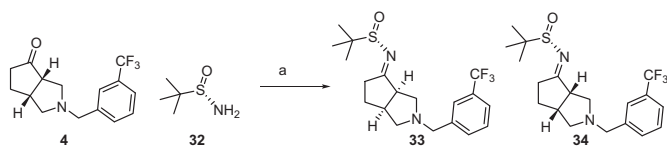
Scheme 2. Reagents and conditions: Ti(OEt)₄, THF, 60 °C, 16 h.



Scheme 3. Reagents and conditions: (a) NaBH₄, MeOH, –78 °C to rt, 16 h; (b) 2N HCl(aq), MeOH, rt, 30 min.



Scheme 4. Reagents and conditions: (a) EDC, HOBT, CH_2Cl_2 , rt, 16 h; (b) 20% $\text{Pd}(\text{OH})_2/\text{carbon}$, MeOH, 30 psi H_2 , rt, 16; (c) PS-CNBH₃, HOAc, CH_2Cl_2 , rt, 16 h.



Scheme 5. Reagents and conditions: $\text{Ti}(\text{OEt})_4$, THF, 60 °C, 16 h.

stereochemistry. Coupling the amine with 2,2-dicyclohexylacetic acid gave the desired enantiomer **37**.

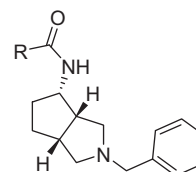
3. Results and discussion

The N-type Ca^{2+} channel activity was determined using IMR32 human neuroblastoma cells that endogenously express the channels, in a functional fluorescent Ca^{2+} flux assay (FLIPR).²⁴ All compounds were also assessed for L-type Ca^{2+} channel activity using a similar FLIPR-based Ca^{2+} flux assay in ND7/23 cells.

Initially, racemic compounds of the structure type shown in Table 1 were screened in the N-type and L-type Ca^{2+} channel assay. This series of compounds blocked N-type Ca^{2+} channels with potencies ranging from 1–3 μM and were generally less potent at L-type Ca^{2+} channels. The first modification made was to replace the N-benzyl substituent with a 3-trifluoromethylbenzyl substituent shown in Table 2. This single modification gave rise to compounds that were approximately fivefold more potent at N-type Ca^{2+} channels. Examples include comparing compound **38** with an IC_{50} value of 4.67 μM to compound **9** with an IC_{50} value of 1.07 μM and compound **39** with an IC_{50} value of 1.46 μM to compound **15** with an IC_{50} value of 0.36 μM .

The amide substituent was also varied to accommodate achiral acids in order to decrease the number of stereocenters in the final product. Not surprisingly, submicromolar potencies were obtained for compounds with more lipophilic amide substituents like bis-cyclohexyl amide **9** with an IC_{50} value of 1.07 μM , diphenyl acetamide **13** with an IC_{50} value of 0.67 μM , and the isopropyl phenyl acetamide **15** with an IC_{50} value of 0.36 μM . In Table 2 the potency to block N-type Ca^{2+} channels increases as lipophilicity increases for smaller substituents. Examples include the cyclopentyl com-

Table 1
 Ca^{2+} channel activity of racemic *n*-benzyl amide analogues



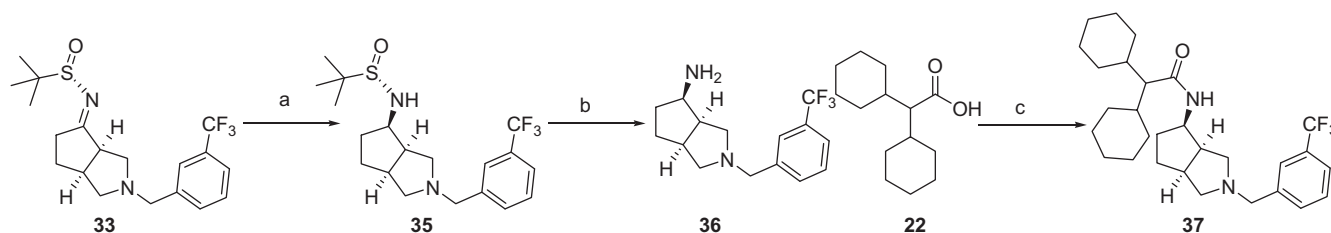
relative stereochemistry (racemic)

Compound R		N-type Ca^{2+} channels		L-type Ca^{2+} channels	
		IC_{50} , μM	$\text{pIC}_{50} \pm \text{SEM}^a$	IC_{50} , μM	$\text{pIC}_{50} \pm \text{SEM}^a$
38	(Cyclohexyl) ₂ CH	4.67	5.33 ± 0.04	>30	
39	(iPr)PhCH	1.46	5.83 ± 0.23	7.21	5.14 ± 0.08
40	(Cyclopentyl) PhCH	0.92	6.03 ± 0.05	5.15	5.29 ± 0.03
41	(Cyclohexyl)PhCH	1.06	5.97 ± 0.17	>30	
42	1-Phenylcyclopentyl	1.93	5.71 ± 0.05	4.84	5.32 ± 0.10
43	1-Phenylcyclohexyl	1.04	5.99 ± 0.05	5.56	5.25 ± 0.03

ound **10** with an IC_{50} value of 2.31 μM , cyclohexyl compound **11** with an IC_{50} value of 1.26 μM and cycloheptyl compound **12** with an IC_{50} value of 0.56 μM . The cyclic and branched acetamides were equipotent: the bis-propyl acetamide **8** with an IC_{50} value of 0.95 μM and cycloheptyl acetamide **12** with an IC_{50} value of 0.56 μM as well as the bis-ethyl **7** with an IC_{50} value of 2.07 μM and cyclopentyl **10** with an IC_{50} value of 2.31 μM .

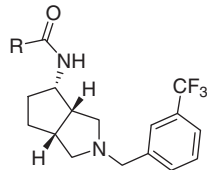
Upon resolving the chirality of the bis-cyclohexyl acetamide analog, we found one enantiomer **25**, the *S,S,R*-4-aminocyclopentapyrrolidine to be 4-fold more potent than the *R,R,S*-4-aminocyclopentapyrrolidine **37** for blocking N-type Ca^{2+} channels (Fig. 2). Further SAR studies were then explored at the *N*-benzyl substituent for this single enantiomer as shown in Table 3. The *meta*- and *para*-substituted aryls were submicromolar in potency. The most potent and selective compound was found to be compound **25**.

The activity of compound **25** was also assessed in a rat aorta ring tissue relaxation assay that measures L-type Ca^{2+} channel activity in native vascular tissue.¹⁷ Compound **25** had an EC_{50} value



Scheme 6. Reagents and conditions: (a) NaBH_4 , MeOH, -78°C to rt, 16 h; (b) 2N HCl(aq), MeOH, rt, 30 min; (c) EDC, HOBT, CH_2Cl_2 , rt, 16 h.

Table 2
Ca²⁺ channel activity of racemic *m*-trifluoromethylbenzyl analogues



relative stereochemistry (racemic)

Compound	R	N-type Ca ²⁺ channels		L-type Ca ²⁺ channels	
		IC ₅₀ μM	pIC ₅₀ ± SEM	IC ₅₀ μM	pIC ₅₀ ± SEM
7	(Ethyl) ₂ CH	2.07	5.68 ± 0.14	19.0	4.72 ± 0.16
8	(Propyl) ₂ CH	0.95	6.02 ± 0.02	20.1	4.69 ± 0.12
9	(Cyclohexyl) ₂ CH	1.07	5.97 ± 0.08	>30	
10	Cyclopentyl	2.31	5.64 ± 0.09	12.8	4.89 ± 0.16
11	Cyclohexyl	1.26	5.90 ± 0.07	16.1	4.79 ± 0.13
12	Cycloheptyl	0.56	6.25 ± 0.11	9.3	4.86 ± 0.17
13	Ph ₂ CH	0.67	6.18 ± 0.06	6.3	5.2 ± 0.05
14	(<i>p</i> -F-Ph) ₂ CH	0.64	6.19 ± 0.08	7.1	5.15 ± 0.06
15	(<i>i</i> Pr)PhCH	0.36	6.45 ± 0.12	5.0	5.3 ± 0.02

All values are means ± SEM of at least three separate experiments.

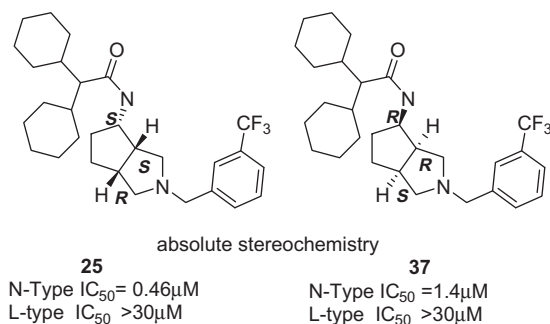
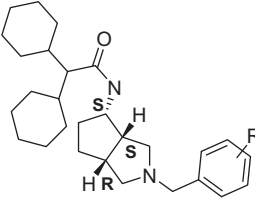


Figure 2. In vitro comparison of enantiomeric pair.

Table 3
Ca²⁺ channel activity of enantiomerically pure *n*-benzyl analogues



absolute stereochemistry

	R	N-type Ca ²⁺ channel		L-type Ca ²⁺ Channel	
		IC ₅₀ , μM ^a	pIC ₅₀ ± SEM ^a	IC ₅₀ , μM ^a	pIC ₅₀ ± SEM ^a
23	H	16.5	4.78 ± 0.07	>30	
26	<i>o</i> -F	1.12	5.95 ± 0.07	>30	
27	<i>m</i> -F	0.99	6.01 ± 0.04	>30	
28	<i>p</i> -F	0.74	6.13 ± 0.06	22.9	4.64 ± 0.04
29	<i>o</i> -CF ₃	2.43	5.61 ± 0.07	>30	
25	<i>m</i> -CF ₃	0.46	6.33 ± 0.06	>30	
30	<i>m</i> -OCF ₃	0.51	6.38 ± 0.05	>30	
31	<i>m</i> -CH ₃	0.86	6.07 ± 0.09	22.3	4.65 ± 0.06

^a All values are means ± SEM of at least three separate experiments.

of 46 μM (95% CI: 10.7–15 nM) compared with the L-type Ca²⁺ channel blocker nifedipine which had a EC₅₀ value of 12 nM (95% CI: 30–71 μM) (Fig. 3).¹⁷

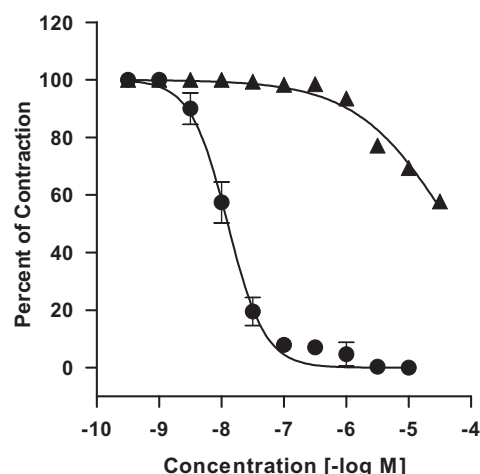


Figure 3. Assessment of Compound **25** in the rat aorta ring tissue relaxation assay. Compound **25** (▲) dose-dependently relaxed KCl-evoked contraction of rat aorta rings. The selective L-type Ca²⁺ channel blocker nifedipine (●) was included as a positive control. Rat aorta rings were precontracted to 1 g tension with 80 mM KCl and the ability of compound **25** to relax the tissue was measured following cumulative additional of the compound over 15 min intervals. The data is presented as % of contraction (*n* = 3).

The activity of compound **25** at N-type Ca²⁺ channels was confirmed using whole cell patch-clamp recordings of rat N-type Ca²⁺ channels overexpressed in HEK293 cells (Fig. 4). Cells were held depolarized to partially inactivate the channels to allow for inhibition of multiple Ca²⁺ channel states to be detected. Under these conditions, compound **25** inhibited N-type Ca²⁺ channels with an IC₅₀ value of 0.041 μM (pIC₅₀ 7.39 ± 0.05). Under more hyperpolarized conditions compound **25** was less potent, inhibiting only 49 ± 6% of the current at 0.3 μM versus 77 ± 6% under inactivating conditions (*p* < 0.05, mean ± SEM, *n* = 5,4 cells, respectively) suggesting that compound **25** blocks N-type Ca²⁺ channels in a state-dependent manner. Although compound **25** was less potent in the FLIPR assay, the electrophysiological assay is a more direct measure of channel inhibition and is assessed at a membrane potential and inactivation level that may not be reflected in the calcium influx FLIPR assay.²⁴

The bis-cyclohexyl moiety, while imparting the desired Ca²⁺ channel activity, contributes to the poor physiochemical properties of these analogs. The aqueous solubility is low (<3 μM) and the plasma protein binding is high (>99%). Additionally the in vitro metabolic stability, determined in incubations with human and rat liver microsomes is low (<5% parent remaining after 30 min). Therefore, compound **25** was assessed in a variety of preclinical pain models following intraperitoneal (ip) dosing where the bioavailability was 41%.

The antinociceptive activity of compound **25** was examined in rat models of carrageenan-induced acute inflammatory, monoiodoacetate-induced osteoarthritis (MIA-OA), and formalin-induced persistent pain. Compound **25** was administered ip 30 min prior to behavioral assessment. In the carrageenan model of acute inflammatory pain, significant thermal hypersensitivity (PWL: 3.1 ± 0.3 s) developed 2 h following carrageenan injection, compared to contralateral side (PWL: 10.8 ± 0.6 s). Compound **25** dose-dependently reversed thermal hypersensitivity, with a maximum effect of 67% at 30 mg/kg (Figure 5A, *p* < 0.01, *n* = 6 per group). In the MIA model of osteoarthritis pain, grip force is reduced (501 ± 50 g) 21 days following MIA injection, compared to the naïve rats (1090 ± 31 g). Compound **25** dose-dependently returned the grip force to normalcy in MIA-OA rats, with a maximum effect of 87% at 30 mg/kg (Figure 5B, *p* < 0.01, *n* = 12 per group). In the formalin model of persistent pain, the formalin injected paw

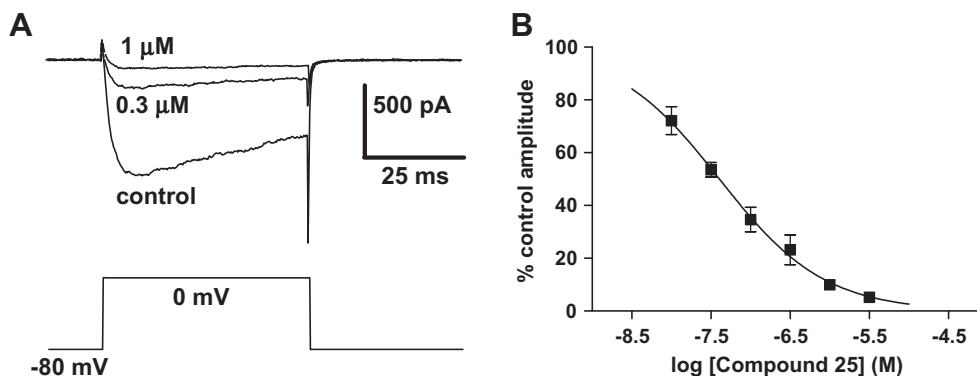


Figure 4. Inhibition of N-type Ca^{2+} channel current by Compound **25** as assessed by manual electrophysiology. (A) Representative current traces illustrating the inhibition of N-type Ca^{2+} channel current by 0.3 μM and 1 μM compound **25** under inactivating conditions as described in the methods. (B) Concentration-response curve for compound **25** yielded an IC_{50} value of 0.041 μM (pIC_{50} 7.39 \pm 0.05). For determining the 50% inhibition concentration (IC_{50}) value, data were fitted to a four parameter logistic equation with the minimum fixed at zero and maximum fixed to 100% of control. $n = 4$ –6 for each data point.

displayed persistent paw flinching behaviors. Compound **25** significantly reduced flinching behavior by 51% at 10 and 30 mg/kg, respectively (Figure 5C, $p < 0.05$, $n = 6$ per group).

In the rat accelerating rotarod assay, compound **25** did not produce rotarod performance deficits at doses up to 30 mg/kg in naïve rats (Figure 6, $p > 0.05$, $n = 6$ per group). In cardiovascular safety studies, compound **25** did not significantly alter hemodynamic function (MAP, HR, or dp/dt) in the anesthetized rat cardiovascular model at plasma concentrations up to 17 $\mu\text{g/ml}$ (10 mg/kg, iv). Based on an EC_{50} plasma concentration in the osteoarthritis pain model of approximately 1 $\mu\text{g/ml}$ (2 μM), compound **25** showed a greater than 15-fold therapeutic margin for antinociception versus cardiovascular liabilities.

4. Conclusion

In conclusion, we have discovered a novel potent N-type calcium channel blocker with selectivity over the L-type Ca^{2+} channel. This compound has analgesic activity in nociceptive pain models without affecting hemodynamic function or motor coordination. These types of compounds are promising new chemical matter for the treatment of pain. Future studies include the discovery of potent and selective N-type Ca^{2+} channel blockers that have enhanced oral bioavailability.

5. Experimental section

5.1. Synthesis

NMR spectra were obtained on Varian M-300, BrukerAMX-400, Varian U-400, or Varian Unity Inova 500 magnetic resonance spectrometers with indicated solvent and tetramethylsilane as the internal standard. Chemical shifts are given in delta (δ) values and coupling constants (J) in Hertz (Hz). The following abbreviations are used for peak multiplicities: s, singlet; d, doublet; t, triplet; q, quartet; m, multiplet; and br, broadened. Standard pulse sequences and phase cycling were used for all correlation spectroscopy (COSY), heteronuclear single-quantum coherence (HSQC), heteronuclear multiple bond coherence (HMBC), and nuclear Overhauser enhancement spectroscopy (NOESY) spectra. ESI (electrospray ionization) mass spectra were performed on a Finnigan SSQ7000 MS run as a flow injection acquisition. All manipulations were performed under nitrogen atmosphere unless otherwise noted. All solvents and reagents were obtained from commercial sources and used without further purification. Silica gel chromatography was carried out using an Analogix® IntelliFlash 280 with

Analogix® cartridges. Elemental analyses were performed by Quantitative Technologies, Inc. Unless otherwise specified, all final compounds were homogeneous with a purity of >95%, as determined by LCMS analysis conducted on a Finnigan Navigator mass spectrometer and Agilent 1100 HPLC system operating under positive APCI ionization conditions. The column used was a Phenomenex® Luna® Combi-HTS C8(2) 5 μm 100 Å° (2.1 \times 30 mm) with a gradient of 10–100% acetonitrile and 0.1% TFA in water or a gradient of 10–100% acetonitrile and 10 mM NH_4OAc in water. Optical rotations were measured with an Autopol IV polarimeter at 20 °C and 589 nm (sodium D line).

5.1.1. *N*-(3-(Trifluoromethyl)benzyl)-1-(trimethylsilyl)methanamine (2)

(3-(Trifluoromethyl)phenyl)methanamine (25 g, 143 mmol), (chloromethyl)trimethylsilane (19.92 mL, 143 mmol), and triethylamine (23.87 mL, 171 mmol) were combined neat and the resultant mixture was refluxed overnight. The reaction was cooled to room temperature and 150 mL of heptane was added. The HCl salts were removed by filtration and washed with heptane. The solvent was removed by placing under house vacuum and then high vacuum. *N*-(3-(Trifluoromethyl)benzyl)-1-(trimethylsilyl)methanamine (29.89 g, 80%) was isolated by vacuum distillation (bp 70–90 °C/3.2 torr): ^1H NMR (300 MHz, CDCl_3) δ ppm 7.59 (s, 1H), 7.53–7.38 (m, 3H), 3.86 (s, 2H), 2.04 (s, 2H), 1.34 (s, 1H), 0.06 (s, 9H).

5.1.2. 1-Methoxy-*N*-(3-(trifluoromethyl)benzyl)-*N*-((trimethylsilyl)methyl)methanamine (3)

Formaldehyde (4.08 g, 50.2 mmol) and methanol (2.032 mL, 50.2 mmol) were combined, and the mixture was cooled to 0 °C (ice bath). *N*-(3-(trifluoromethyl)benzyl)-1-(trimethylsilyl)methanamine (10.94 g, 41.9 mmol) was added dropwise via addition funnel over 30 min. Potassium carbonate (4.63 g, 33.5 mmol) was added, and the reaction stirred at 0 °C for 2 additional hours. The reaction product was decanted from the potassium carbonate, treated with more potassium carbonate, and decanted again. The potassium carbonate solids were washed several times with ether, and these washes were added to the product solution. The solvent was removed in vacuo to give 1-methoxy-*N*-(3-(trifluoromethyl)benzyl)-*N*-((trimethylsilyl)methyl)methanamine (12.33 g, 96%) which was used directly in the next step.

5.1.3. 2-(3-(Trifluoromethyl)benzyl)hexahydrocyclopenta[*c*]pyrrol-4(5H)-one (4)

Cyclopent-2-enone (3.31 g, 40.4 mmol) and trifluoroacetic acid (0.031 mL, 0.404 mmol) were combined in dichloromethane

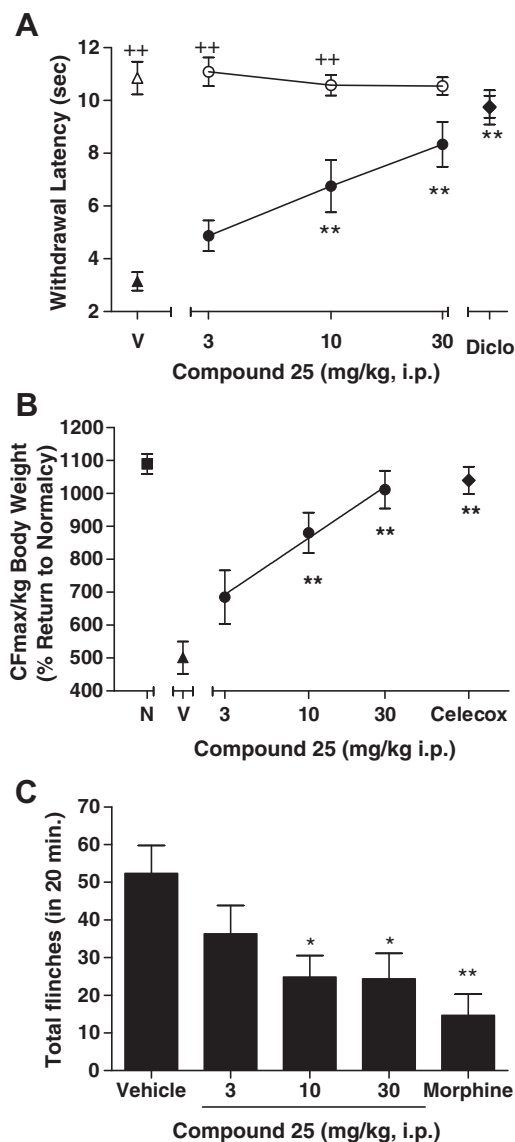


Figure 5. Antinociceptive effects of compound **25** on inflammatory, osteoarthritic and persistent pain. Compound **25** (3, 10 and 30 mg/kg) was administered ip 30 min prior to behavioral assessment in each pain model. (A) Effect of compound **25** on carrageenan-induced inflammatory thermal hypersensitivity. Paw withdrawal latency (PWL) was measured 2 h following carrageenan injection of right hind paw. Diclo: diclofenac (30 mg/kg, ip) as positive control. (B) Effect of compound **25** on MIA-induced osteoarthritic pain. Grip force was assessed at least 21 days after MIA-injection. V: vehicle; N: naïve; Celecox: celecoxib (30 mg/kg, ip) as positive control. (C) Compound **25** on formalin-induced persistent pain. Paw flinching was assessed for a period of 20 min (30–50 min following formalin injection, that is, phase II). Data are shown as mean \pm SEM. * p < 0.05, ** p < 0.01, compared to vehicle-treated rats (n = 6–12 per group).

(40 mL). 1-Methoxy-*N*-(3-(trifluoromethyl)benzyl)-*N*-((trimethylsilyl)methyl)methanamine (12.33 g, 40.4 mmol) was added as a solution in 10 mL of dichloromethane dropwise via addition funnel over 45 min at room temperature under nitrogen. The reaction was quenched with aqueous sodium bicarbonate and extracted with 2 \times 100 mL of dichloromethane. The organic washes were combined and washed with brine. The solvent was removed in vacuo to give 2-(3-(trifluoromethyl)benzyl)hexahydrocyclopenta[*c*]pyrrol-4(5*H*)-one (11.7 g, 100%): ^1H NMR (300 MHz, CDCl_3) δ ppm 7.54–7.34 (m, 4H), 3.66 (d, J = 13.4, 1H), 3.52 (d, J = 13.4, 1H), 3.04 (dd, J = 1.8, 8.9, 1H), 2.91 (ddd, J = 2.8, 7.4, 11.7, 1H), 2.72–2.65 (m, 1H), 2.62 (d, J = 8.9, 1H), 2.52–2.23 (m, 4H), 2.15 (ddd, J = 8.1, 12.9, 17.1, 1H), 1.85–1.70 (m, 1H); MS (ESI+) m/z 284 (M+H) $^+$.

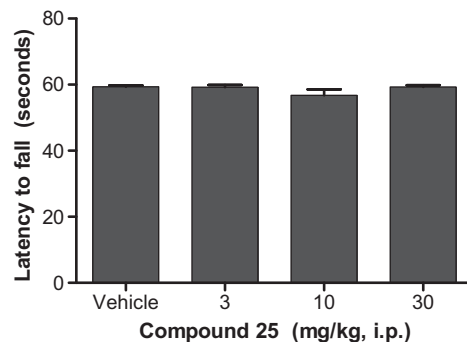


Figure 6. The effect of compound **25** on Rotarod performance in naïve rats. Compound **25** (3, 10 and 30 mg/kg) was administered i.p., fall latency (seconds) was assessed 30 min after compound treatment in the accelerating rotarod assay. Data are shown as mean \pm SEM (n = 6 per group).

5.1.4. 2-(3-(Trifluoromethyl)benzyl)hexahydrocyclopenta[*c*]pyrrol-4(5*H*)-one oxime (**5**)

Hydroxylamine hydrochloride (3.47 g, 50.0 mmol) and sodium acetate (4.27 g, 52.0 mmol) were dissolved in 15 mL of water and added to a solution of 2-(3-(trifluoromethyl)benzyl)hexahydrocyclopenta[*c*]pyrrol-4(5*H*)-one (11.33 g, 40 mmol) in ethanol (80 mL). The reaction was brought to reflux for 5 min and allowed to cool to 70 $^\circ\text{C}$. After 1 h, the reaction mixture was cooled, and the solvent was removed in vacuo to give 2-(3-(trifluoromethyl)benzyl)hexahydrocyclopenta[*c*]pyrrol-4(5*H*)-one oxime (11.93 g, 100%) which was used without additional purification in the next step; MS (ESI+) m/z 299 (M+H) $^+$.

5.1.5. (3*aS**,4*S**,6*aR**)-2-(3-(Trifluoromethyl)benzyl)octahydrocyclopenta[*c*]pyrrol-4-amine (**6**)

2-(3-(Trifluoromethyl)benzyl)hexahydrocyclopenta[*c*]pyrrol-4(5*H*)-one oxime (11.9 g, 39.9 mmol) in 20% ammonia-methanol (115 mL) was added to methanol-washed Raney $^{\text{®}}$ -nickel, (water-wet, 38.52 g, 295 mmol) in a 500 mL pressure bottle. The vessel was pressurized with hydrogen (30 psi), and the mixture was shaken for 16 h at ambient temperature. The mixture was filtered through a nylon membrane, the solvent was removed in vacuo, and the crude material was adsorbed onto silica gel. Silica gel chromatography using a 400 g silica gel cartridge eluting with 1–10% methanol (2*N* ammonia)/dichloromethane gave the following diastereomers: (3*aS**,4*S**,6*aR**)-2-(3-(trifluoromethyl)benzyl)octahydrocyclopenta[*c*]pyrrol-4-amine (**6**) (3.946 g, 35%): ^1H NMR (300 MHz, pyridine- d_5) δ ppm 7.58 (s, 1H), 7.50 (t, J = 7.2, 2H), 7.45–7.37 (m, 1H), 3.59 (s, 2H), 3.09 (dd, J = 4.9, 11.4, 1H), 2.77–2.57 (m, J = 3.9, 1H), 2.52–2.38 (m, 3H), 2.34 (dd, J = 3.7, 9.0, 1H), 2.22–2.09 (m, 1H), 2.03–1.85 (m, J = 4.7, 7.0, 10.8, 2H), 1.42–1.21 (m, 4H); MS (ESI+) m/z 285 (M+H) $^+$ and (3*aS**,4*R**,6*aR**)-2-(3-(trifluoromethyl)benzyl)octahydrocyclopenta[*c*]pyrrol-4-amine (2.99 g, 26%): ^1H NMR (300 MHz, pyridine- d_5) δ ppm 7.58 (s, 1H), 7.50 (t, J = 6.7, 2H), 7.45–7.37 (m, 1H), 3.59 (s, 2H), 3.26 (dt, J = 6.3, 12.6, 1H), 2.67–2.50 (m, 4H), 2.38 (dd, J = 6.6, 8.4, 1H), 2.31–2.20 (m, 1H), 1.79–1.62 (m, 2H), 1.60–1.33 (m, 4H); MS (ESI+) m/z 285 (M+H) $^+$.

5.1.6. (*R,E*)-*N*-((3*aR*,6*aS*)-2-Benzylhexahydrocyclopenta[*c*]pyrrol-4(5*H*)-ylidene)-2-methylpropane-2-sulfinamide (**18**) and (*R,E*)-*N*-((3*aS*,6*aR*)-2-benzylhexahydrocyclopenta[*c*]pyrrol-4(5*H*)-ylidene)-2-methylpropane-2-sulfinamide (**19**)

2-Benzylhexahydrocyclopenta[*c*]pyrrol-4(5*H*)-one (8.88 g, 41.3 mmol), titanium tetrathoxide (18.82, 83 mmol), and (*R*)-2-methylpropane-2-sulfinamide (5.00 g, 41.3 mmol) were combined in tetrahydrofuran (138 mL). The reaction was heated at 60 $^\circ\text{C}$

overnight. The reaction was then reduced in volume to about half and poured into 75 mL of saturated aqueous ammonium chloride. The precipitate was collected by filtration and washed with ethyl acetate. The filtrate was poured into a separatory funnel and the organic layer was removed. The aqueous layer was extracted with ethyl acetate (3 × 200 mL). The organic washes were combined and washed with brine, dried (Na₂SO₄) and concentrated. The crude material was chromatographed using silica gel cartridge (Analogix, RS65–400) eluting with 5–100% ethyl acetate/hexanes to give (*R,E*)-*N*-((3*aS*,6*aS*)-2-benzylhexahydrocyclopenta[*c*]pyrrol-4(5*H*)-ylidene)-2-methylpropane-2-sulfinamide (**18**) (4.12 g, 31% yield) and (*R,E*)-*N*-((3*aS*,6*aR*)-2-benzylhexahydrocyclopenta[*c*]pyrrol-4(5*H*)-ylidene)-2-methylpropane-2-sulfinamide (**19**) (2.88 g, 22% yield).

5.1.7. (*R*)-*N*-((3*aS*,4*S*,6*aR*)-2-Benzyl-octahydrocyclopenta[*c*]pyrrol-4-yl)-2-methylpropane-2-sulfinamide (**20**)

A mixture of (*R,E*)-*N*-((3*aS*,6*aR*)-2-benzylhexahydrocyclopenta[*c*]pyrrol-4(5*H*)-ylidene)-2-methylpropane-2-sulfinamide **18** (4.128 g, 12.96 mmol) in methanol (40 mL) was cooled to –78 °C in a dry ice/acetone bath. Sodium borohydride (1.471 g, 38.9 mmol) was added, and the reaction was allowed to warm to room temperature overnight. The reaction was quenched with saturated aqueous ammonium chloride, diluted with water, and extracted with 3 × 100 mL of ethyl acetate. The extracts were dried (Na₂SO₄) and filtered. The solvent was removed in vacuo to give (*R*)-*N*-((3*aS*,4*S*,6*aR*)-2-benzyl-octahydrocyclopenta[*c*]pyrrol-4-yl)-2-methylpropane-2-sulfinamide **20** (4.50 g, 100% yield) as a yellow crystalline solid: ¹H NMR (500 MHz, pyridine-*d*₅) δ ppm 7.39 (dt, *J* = 13.1, 7.3, 4H), 7.30 (t, *J* = 7.2, 1H), 5.15 (d, *J* = 7.4, 1H), 3.80–3.72 (m, 1H), 3.51 (s, 2H), 2.86 (dd, *J* = 9.4, 3.6, 1H), 2.65 (qd, *J* = 7.9, 3.6, 1H), 2.46–2.35 (m, 2H), 2.32–2.25 (m, 2H), 2.06 (ddd, *J* = 14.7, 12.1, 7.8, 1H), 1.69 (td, *J* = 11.9, 5.9, 1H), 1.63–1.54 (m, 1H), 1.38–1.29 (m, 1H), 1.19 (s, 9H); MS (ESI+) *m/z* 321(M+H)⁺.

5.1.8. (3*aS*,4*S*,6*aR*)-2-Benzyl-octahydrocyclopenta[*c*]pyrrol-4-amine (**21**)

(*R*)-*N*-((3*aS*,4*S*,6*aR*)-2-Benzyl-octahydrocyclopenta[*c*]pyrrol-4-yl)-2-methylpropane-2-sulfinamide **20** (4.15 g, 12.95 mmol) and 2 *N*HCl (10 mL, 40.0 mmol) were combined in methanol (10 mL). After 30 min, the solvent was removed and the crude material was purified on a silica gel cartridge (Analogix, RS-40) loading with 10% methanol (2 *N* ammonia)/dichloromethane solution and eluting with 2–10% methanol (2 *N* ammonia)/dichloromethane to give (3*aS*,4*S*,6*aR*)-2-benzyl-octahydrocyclopenta[*c*]pyrrol-4-amine **21** (2.69 g, 96% yield): ¹H NMR (500 MHz, pyridine-*d*₅) δ ppm 7.44 (d, *J* = 7.4, 2H), 7.36 (t, *J* = 7.5, 2H), 7.28 (t, *J* = 7.3, 1H), 3.52 (q, *J* = 13.0, 2H), 3.29 (q, *J* = 7.3, 1H), 2.84 (dd, *J* = 3.7, 9.3, 1H), 2.55–2.43 (m, 3H), 2.37–2.30 (m, 1H), 2.24 (d, *J* = 5.3, 1H), 1.74–1.64 (m, 2H), 1.62–1.53 (m, 1H), 1.34 (dd, *J* = 5.0, 10.1, 1H); MS (ESI+) *m/z* 217(M+H)⁺.

5.1.9. 2,2-Dicyclohexyl-*N*-[(3*aS*,4*S*,6*aR*)-octahydrocyclopenta[*c*]pyrrol-4-yl]acetamide (**24**)

N-[(3*aS*,4*S*,6*aR*)-2-Benzyl-octahydrocyclopenta[*c*]pyrrol-4-yl]-2,2-dicyclohexylacetamide (2.65 g, 6.27 mmol) **23** and methanol 60 mL were added to 20% palladium hydroxide on carbon, (wet, 0.530 g, 3.77 mmol) in a 250 mL pressure bottle. The reaction was stirred for 16 h under hydrogen (30 psi) at room temperature. The mixture was filtered through a nylon membrane and the solvent removed in vacuo. The crude material was chromatographed on a silica gel cartridge (Analogix, RS25–25) eluting with 1–10% methanol (2 *N* ammonia)/dichloromethane to give 2,2-dicyclohexyl-*N*-[(3*aS*,4*S*,6*aR*)-octahydrocyclopenta[*c*]pyrrol-4-yl]acetamide **24** (1.69 g, 81% yield): ¹H NMR (500 MHz, pyridine-*d*₅) δ ppm 7.97 (d, *J* = 7.1, 1H), 4.57 (dt, *J* = 7.0, 13.8, 1H), 3.03 (dd, *J* = 3.2,

10.1, 1H), 2.89 (dd, *J* = 7.8, 9.7, 1H), 2.78 (dd, *J* = 7.4, 10.1, 1H), 2.71 (ddd, *J* = 3.2, 7.5, 16.7, 1H), 2.58 (dd, *J* = 3.2, 9.8, 1H), 2.50–2.39 (m, *J* = 8.3, 1H), 1.98–1.89 (m, 3H), 1.89–1.80 (m, 3H), 1.79–1.67 (m, *J* = 6.4, 14.9, 7H), 1.66–1.56 (m, 3H), 1.49–1.36 (m, 2H), 1.36–1.28 (m, 1H), 1.28–1.02 (m, 8H); MS (ESI+) *m/z* 333 (M+H)⁺.

5.2. General procedure for reductive alkylation for compounds 25–31

5.2.1. 2,2-Dicyclohexyl-*N*-[(3*aS*,4*S*,6*aR*)-2-[3-(trifluoromethyl)benzyl]octahydrocyclopenta[*c*]pyrrol-4-yl]acetamide (**25**)

2,2-Dicyclohexyl-*N*-[(3*aS*,4*S*,6*aR*)-octahydrocyclopenta[*c*]pyrrol-4-yl]acetamide (154 mg, 0.463 mmol) **24** and 3-(trifluoromethyl)benzaldehyde (0.062 mL, 0.463 mmol) were combined in dichloromethane (5 mL), and then 2 mL of acetic acid was added. The reaction was stirred at room temperature for 20 min, and then PS-cyanoborohydride (396 mg, 0.926 mmol) was added. The reaction was stirred at room temperature overnight, then filtered and the resin was washed with dichloromethane. The solvent was removed in vacuo, and the crude material was purified using a silica gel cartridge (Analogix, RS-25) eluting with 1–10% methanol (2*N* ammonia)/dichloromethane to give 2,2-dicyclohexyl-*N*-[(3*aS*,4*S*,6*aR*)-2-[3-(trifluoromethyl)benzyl]octahydrocyclopenta[*c*]pyrrol-4-yl]acetamide **25** (160 mg, 70% yield): [α]_D²⁰ –70.2° (c 1.03, CH₃OH). ¹H NMR (500 MHz, pyridine-*d*₅) δ ppm 7.73 (s, 1H), 7.66 (d, *J* = 7.7, 1H), 7.56 (s, 1H), 7.50 (t, *J* = 7.7, 1H), 4.51–4.43 (m, 1H), 3.55 (d, *J* = 12.9, 1H), 3.46 (d, *J* = 12.9, 1H), 2.75 (d, *J* = 8.6, 2H), 2.52–2.41 (m, *J* = 8.5, 19.1, 2H), 2.34–2.29 (m, 1H), 2.20 (dd, *J* = 7.7, 9.8, 1H), 2.14 (s, 3H, OAc), 1.96–1.54 (m, 15H), 1.49–1.05 (m, 12H), 1.03–0.93 (m, *J* = 11.7, 21.1, 1H); MS (ESI+) *m/z* 491 (M+H)⁺; Anal. (C₂₉H₄₁F₃N₂O) C, H, N.

5.2.2. 2,2-Dicyclohexyl-*N*-[(3*aS*,4*S*,6*aR*)-2-(2-fluorobenzyl)octahydrocyclopenta[*c*]pyrrol-4-yl]acetamide (**26**)

(89 mg, 56% yield): ¹H NMR (500 MHz, pyridine-*d*₅) δ ppm 7.55 (s, 1H), 7.36 (dt, *J* = 6.6, 24.8, 2H), 7.20–7.15 (m, 2H), 4.44 (s, 1H), 3.68 (d, *J* = 12.6, 1H), 3.44 (d, *J* = 12.6, 1H), 2.77 (d, *J* = 9.6, 1H), 2.64 (dd, *J* = 7.5, 15.0, 1H), 2.53 (d, *J* = 9.0, 1H), 2.49–2.40 (m, 1H), 2.29 (t, *J* = 8.3, 1H), 2.16–2.09 (m, 1H), 1.98–1.64 (m, 12H), 1.61 (d, *J* = 11.4, 2H), 1.55–1.37 (m, *J* = 13.8, 20.5, 31.3, 3H), 1.34–1.08 (m, 9H), 1.00 (dd, *J* = 13.4, 22.1, 1H); MS (ESI+) *m/z* 441 (M+H)⁺; Anal. (C₂₈H₄₁FN₂O·1HCl·2.2H₂O) C, H, N.

5.2.3. 2,2-Dicyclohexyl-*N*-[(3*aS*,4*S*,6*aR*)-2-(3-fluorobenzyl)octahydrocyclopenta[*c*]pyrrol-4-yl]acetamide (**27**)

(84 mg, 53% yield): ¹H NMR (500 MHz, pyridine-*d*₅) δ ppm 7.36 (dd, *J* = 7.8, 13.9, 1H), 7.19–7.11 (m, 3H), 4.49–4.42 (m, 1H), 3.55 (d, *J* = 12.8, 1H), 3.34 (d, *J* = 12.8, 1H), 2.78–2.69 (m, *J* = 8.0, 15.6, 2H), 2.51–2.43 (m, *J* = 10.6, 2H), 2.29 (t, *J* = 8.4, 1H), 2.13 (dd, *J* = 7.2, 9.5, 1H), 1.97–1.77 (m, 7H), 1.77–1.64 (m, 5H), 1.63–1.47 (m, 4H), 1.42 (ddd, *J* = 3.0, 12.2, 23.0, 1H), 1.33 (dd, *J* = 9.7, 23.2, 1H), 1.29–1.08 (m, 8H), 1.02 (dd, *J* = 11.8, 22.6, 1H); MS (ESI+) *m/z* 441 (M+H)⁺; Anal. (C₂₈H₄₁FN₂O·1HCl·1.7H₂O) C, H, N.

5.2.4. 2,2-Dicyclohexyl-*N*-[(3*aS*,4*S*,6*aR*)-2-(4-fluorobenzyl)octahydrocyclopenta[*c*]pyrrol-4-yl]acetamide (**28**)

(103 mg, 65% yield): ¹H NMR (500 MHz, pyridine-*d*₅) δ ppm 7.54 (d, *J* = 6.0, 1H), 7.40–7.29 (m, 2H), 7.18 (d, *J* = 8.7, 2H), 4.53–4.38 (m, 1H), 3.55 (d, *J* = 12.5, 1H), 3.29 (d, *J* = 12.6, 1H), 2.72 (dd, *J* = 8.6, 17.7, 2H), 2.56–2.39 (m, 2H), 2.29 (t, *J* = 8.3, 1H), 2.10 (t, *J* = 8.1, 1H), 1.98–1.07 (m, 26H), 0.99 (dd, *J* = 10.2, 22.0, 1H); MS (ESI+) *m/z* 441 (M+H)⁺; Anal. (C₂₈H₄₁FN₂O·1HCl·3.0H₂O) C, H, N.

5.2.5. 2,2-Dicyclohexyl-*N*-[(3*aS*,4*S*,6*aR*)-2-[2-(trifluoromethyl)benzyl]octahydrocyclopenta[*c*]pyrrol-4-yl]acetamide (**29**)

(72 mg, 44% yield): ¹H NMR (500 MHz, pyridine-*d*₅) δ ppm 7.74 (d, *J* = 7.8, 1H), 7.64 (d, *J* = 7.7, 1H), 7.55 (d, *J* = 7.6, 1H), 7.43 (dd,

$J = 7.0, 13.9, 2\text{H}$), 4.51–4.43 (m, 1H), 3.82 (d, $J = 13.7, 1\text{H}$), 3.54 (d, $J = 13.7, 1\text{H}$), 2.81–2.70 (m, 2H), 2.53–2.43 (m, 2H), 2.35 (t, $J = 8.1, 1\text{H}$), 2.23–2.17 (m, 1H), 1.95–1.68 (m, 10H), 1.67–1.52 (m, 5H), 1.46–1.04 (m, 11H), 0.97–0.86 (m, 1H); MS (ESI+) m/z 491 (M+H)⁺; Anal. (C₂₉H₄₁F₃N₂O·1HCl·1.7H₂O) C, H, N.

5.2.6. 2,2-Dicyclohexyl-*N*-((3*aS*,4*S*,6*aR*)-2-(3-(trifluoromethyl)benzyl)octahydrocyclopenta[c]pyrrol-4-yl)acetamide (30)

(109 mg, 60% yield): ¹H NMR (500 MHz, pyridine-*d*₅) δ ppm 7.60 (d, $J = 7.3, 1\text{H}$), 7.42 (t, $J = 7.9, 1\text{H}$), 7.37 (s, 1H), 7.30 (dd, $J = 7.9, 16.8, 2\text{H}$), 4.51–4.44 (m, 1H), 3.50 (d, $J = 13.0, 1\text{H}$), 3.45 (d, $J = 13.0, 1\text{H}$), 2.80–2.72 (m, $J = 4.8, 16.2, 2\text{H}$), 2.51–2.42 (m, $J = 8.7, 2\text{H}$), 2.29 (t, $J = 8.3, 1\text{H}$), 2.20 (dd, $J = 7.2, 9.2, 1\text{H}$), 1.96–1.89 (m, 2H), 1.89–1.78 (m, 4H), 1.77–1.65 (m, 5H), 1.64–1.51 (m, 4H), 1.42 (dd, $J = 9.4, 23.0, 1\text{H}$), 1.36–1.09 (m, 10H), 1.08–0.98 (m, 1H); MS (ESI+) m/z 507 (M+H)⁺; Anal. (C₂₉H₄₁F₃N₂O₂·1HCl·2.6H₂O) C, H, N.

5.2.7. 2,2-Dicyclohexyl-*N*-[(3*aS*,4*S*,6*aR*)-2-(3-methylbenzyl)octahydrocyclopenta[c]pyrrol-4-yl]acetamide (31)

(126 mg, 80% yield): ¹H NMR (500 MHz, pyridine-*d*₅) δ ppm 7.53 (d, $J = 5.8, 1\text{H}$), 7.32 (t, $J = 7.5, 1\text{H}$), 7.24–7.22 (m, 1H), 7.20–7.14 (m, 2H), 4.50–4.42 (m, 1H), 3.57 (d, $J = 12.4, 1\text{H}$), 3.34 (d, $J = 12.3, 1\text{H}$), 2.78 (d, $J = 9.4, 1\text{H}$), 2.66 (dd, $J = 7.5, 15.1, 1\text{H}$), 2.55 (d, $J = 8.8, 1\text{H}$), 2.50–2.42 (m, 1H), 2.33 (s, 3H), 2.31–2.24 (m, 1H), 2.14–2.07 (m, 1H), 1.98–1.57 (m, 13H), 1.53 (ddd, $J = 6.4, 11.9, 18.4, 1\text{H}$), 1.42 (t, $J = 10.0, 2\text{H}$), 1.38–1.08 (m, 10H), 1.02–0.92 (m, 1H); MS (ESI+) m/z 437 (M+H)⁺; Anal. (C₂₉H₄₄N₂O·1HCl·2.6H₂O) C, H, N.

5.2.8. (*S,E*)-2-Methyl-*N*-((3*aR*,6*aS*)-2-(3-(trifluoromethyl)benzyl)hexahydrocyclopenta[c]pyrrol-4(5*H*)-ylidene)propane-2-sulfinamide (33) and (*S,E*)-2-methyl-*N*-((3*aS*,6*aR*)-2-(3-(trifluoromethyl)benzyl)hexahydrocyclopenta[c]pyrrol-4(5*H*)-ylidene)propane-2-sulfinamide (34)

2-(3-(Trifluoromethyl)benzyl) hexahydrocyclopenta[c]pyrrol-4(5*H*)-one **4** (3.672 g, 12.96 mmol), titanium tetraethoxide (5.11 ml, 24.63 mmol), and (*S*)-2-methylpropane-2-sulfinamide (1.885 g, 15.55 mmol) were combined in THF (200 ml) to give an orange solution. The reaction was heated at 60 °C overnight to give a brown solution. The reaction was then reduced in volume to about half and poured into 75 mL brine and filtered, washing the dark pink precipitate with EtOAc. The filtrate was poured into a separatory funnel and the organics removed and the solvent reduced in volume. The crude material was chromatographed using an RS65–200 with 5–100% EtOAc/hexanes to give (*S,E*)-2-methyl-*N*-((3*aR*,6*aS*)-2-(3-(trifluoromethyl)benzyl)hexahydrocyclopenta[c]pyrrol-4(5*H*)-ylidene)propane-2-sulfinamide (**33**) (1.327 g, 26% yield): MS (ESI+) m/z 387 (M+H)⁺ and (*S,E*)-2-methyl-*N*-((3*aS*,6*aR*)-2-(3-(trifluoromethyl)benzyl)hexahydrocyclopenta[c]pyrrol-4(5*H*)-ylidene)propane-2-sulfinamide (**34**) (1.188 g, 24% yield): ¹H NMR (300 MHz, CDCl₃) δ ppm 7.57–7.36 (m, 5H), 3.59 (s, 2H), 3.13–2.99 (m, 1H), 2.98–2.62 (m, 4H), 2.57–2.43 (m, 2H), 2.12 (ddd, $J = 16.9, 13.2, 8.2, 1\text{H}$), 1.84–1.69 (m, 1H), 1.19 (s, 9H); MS (ESI+) m/z 387 (M+H)⁺.

5.2.9. (*S*)-2-Methyl-*N*-((3*aR*,4*R*,6*aS*)-2-(3-(trifluoromethyl)benzyl)octahydrocyclopenta[c]pyrrol-4-yl)propane-2-sulfinamide (35)

(*S,E*)-2-Methyl-*N*-((3*aR*,6*aS*)-2-(3-(trifluoromethyl)benzyl)hexahydrocyclopenta[c]pyrrol-4(5*H*)-ylidene)propane-2-sulfinamide **33** (1.327 g, 3.43 mmol) in MeOH (25 mL) was cooled to –78 °C in a dry ice/acetone bath to give a yellow solution. NaBH₄ (0.390 g, 10.30 mmol) was added and the reaction was allowed to warm to ambient temperature overnight. The reaction was quenched with ammonium chloride, diluted with water, and extracted with 3 × 100 mL of ethyl acetate. The extracts were dried (Na₂SO₄) and filtered. The solvent was removed in vacuo and the crude material chromatographed using an RS-40 with 5–50% acetone/

hexanes to give (*S*)-2-methyl-*N*-((3*aR*,4*R*,6*aS*)-2-(3-(trifluoromethyl)benzyl)octahydrocyclopenta[c]pyrrol-4-yl)propane-2-sulfinamide (**35**) (975 mg, 73% yield) as a pale yellow oil: ¹H NMR (500 MHz, pyridine-*d*₅) δ ppm 7.75 (s, 1H), 7.60 (d, $J = 7.9, 2\text{H}$), 7.46 (t, $J = 7.7, 1\text{H}$), 5.18 (d, $J = 6.8, 1\text{H}$), 3.81–3.73 (m, 1H), 3.54 (s, 2H), 2.86 (dd, $J = 9.4, 3.9, 1\text{H}$), 2.72–2.65 (m, 1H), 2.48–2.39 (m, 2H), 2.32 (dd, $J = 9.2, 7.9, 1\text{H}$), 2.27 (d, $J = 5.5, 1\text{H}$), 2.07–1.98 (m, 1H), 1.70 (dt, $J = 11.6, 5.7, 1\text{H}$), 1.64–1.53 (m, 1H), 1.32 (dd, $J = 15.8, 5.3, 1\text{H}$), 1.18 (s, 9H). MS (ESI+) m/z 389 (M+H)⁺.

5.2.10. (3*aR*,4*R*,6*aS*)-2-(3-(Trifluoromethyl)benzyl)octahydrocyclopenta[c]pyrrol-4-amine (36)

(*S*)-2-Methyl-*N*-((3*aR*,4*R*,6*aS*)-2-(3-(trifluoromethyl)benzyl)octahydrocyclopenta[c]pyrrol-4-yl)propane-2-sulfinamide **35** (765 mg, 1.969 mmol) dissolved in 4 N HCl in dioxane (10 mL, 40.0 mmol) and MeOH (10 mL) to give a yellow solution. After 30 min the solvent was removed and the crude material purified (loaded on with methanol (2N ammonia) using a 24 g silica gel cartridge and 2–10% methanol (2 N ammonia)/dichloromethane to give (3*aR*,4*R*,6*aS*)-2-(3-(trifluoromethyl)benzyl)octahydrocyclopenta[c]pyrrol-4-amine (**36**) (492 mg, 88% yield): ¹H NMR (500 MHz, pyridine-*d*₅) δ ppm 7.78 (s, 1H), 7.59 (d, $J = 11.1, 2\text{H}$), 7.45 (t, $J = 7.7, 1\text{H}$), 4.94 (br s, 2H), 3.14 (dd, $J = 5.2, 11.5, 1\text{H}$), 2.58 (tt, $J = 5.1, 10.1, 1\text{H}$), 2.49 (dd, $J = 3.3, 9.0, 1\text{H}$), 2.35 (dd, $J = 7.5, 9.0, 1\text{H}$), 2.31 (d, $J = 5.8, 2\text{H}$), 2.21–2.14 (m, 1H), 2.00–1.92 (m, 1H), 1.88 (td, $J = 4.2, 9.9, 1\text{H}$), 1.39–1.29 (m, 2H); MS (ESI+) m/z 284 (M+H)⁺.

5.3. General procedure for amide synthesis 38–43, 7–15, 23, 37

5.3.1. *N*-[(3*aS**,4*S**,6*aR**)-2-Benzyloctahydrocyclopenta[c]pyrrol-4-yl]-2,2-dicyclohexylacetamide (38)

(3*aS**,6*aR**)-2-Benzyloctahydrocyclopenta[c]pyrrol-4-amine (500 mg, 2.311 mmol), 2,2-dicyclohexylacetic acid (570 mg, 2.54 mmol), and 1-hydroxybenzotriazole (389 mg, 2.54 mmol) were combined in dichloromethane (20 mL). The reaction was stirred at room temperature for 10 min, then *N*-(3-dimethylamino-propyl)-*N*-ethylcarbodiimide (0.449 mL, 2.54 mmol) was added dropwise. The reaction was stirred at room temperature for 20 h, and then the reaction was quenched with 10 mL of water. The reaction was extracted with 2 × 20 mL of dichloromethane, the solvent was removed in vacuo, and the crude material was chromatographed over a 40 g silica gel cartridge eluting with 30–50% ethyl acetate/hexanes to give *N*-[(3*aS**,4*S**,6*aR**)-2-benzyloctahydrocyclopenta[c]pyrrol-4-yl]-2,2-dicyclohexylacetamide (299 mg, 0.707 mmol, 30% yield): ¹H NMR (500 MHz, pyridine-*d*₅) δ ppm 7.60 (d, $J = 5.1, 1\text{H}$), 7.45–7.38 (m, 4H), 7.35 (m, 1H), 4.49–4.41 (m, 1H), 3.57 (d, $J = 12.6, 1\text{H}$), 3.37 (d, $J = 12.5, 1\text{H}$), 2.76 (d, $J = 9.6, 1\text{H}$), 2.69 (dd, $J = 7.9, 15.7, 1\text{H}$), 2.50 (d, $J = 9.1, 1\text{H}$), 2.48–2.41 (m, 1H), 2.28 (t, $J = 8.2, 1\text{H}$), 2.15–2.08 (m, 1H), 1.99–1.06 (m, 26H), 1.04–0.92 (m, 1H); MS (ESI+) m/z 423 (M+H)⁺; Anal. (C₂₈H₄₂N₂O) C, H, N.

5.3.2. *N*-[(3*aR**,4*R**,6*aS**)-2-Benzyloctahydrocyclopenta[c]pyrrol-4-yl]-3-methyl-2-phenylbutanamide (39)

(22.6 mg, 23% yield): ¹H NMR (500 MHz, pyridine-*d*₅) δ ppm 8.13–8.03 (m, 1H), 7.65 (d, $J = 7.2, 1\text{H}$), 7.55 (d, $J = 7.3, 1\text{H}$), 7.44 (d, $J = 4.3, 2\text{H}$), 7.41 (d, $J = 7.0, 1\text{H}$), 7.36 (t, $J = 6.9, 3\text{H}$), 7.28 (ddd, $J = 7.3, 14.7, 17.5, 2\text{H}$), 4.40 (dd, $J = 6.7, 13.3, 0.5\text{H}$), 4.35–4.27 (m, 0.5H), 3.55 (d, $J = 12.7, 0.5\text{H}$), 3.40 (dd, $J = 4.5, 12.8, 1\text{H}$), 3.26 (d, $J = 12.9, 0.5\text{H}$), 3.16 (d, $J = 10.5, 0.5\text{H}$), 3.05 (d, $J = 10.5, 0.5\text{H}$), 2.78 (dd, $J = 8.1, 15.8, 1\text{H}$), 2.69–2.54 (m, 1.5H), 2.43–2.26 (m, 3H), 2.23–2.13 (m, 1H), 1.94–1.82 (m, 1H), 1.73–1.57 (m, 1.5H), 1.50 (dt, $J = 7.1, 15.0, 0.5\text{H}$), 1.38 (td, $J = 6.4, 12.2, 0.5\text{H}$), 1.27 (m, 0.5H), 1.19 (d, $J = 6.4, 1.5\text{H}$), 1.11 (dd, $J = 5.7, 12.0, 0.5\text{H}$), 1.03 (d, $J = 6.5, 1.5\text{H}$), 0.73 (dd, $J = 6.7, 10.7, 3\text{H}$); MS (ESI+) m/z 377 (M+H)⁺; Anal. (C₂₅H₃₂N₂O·0.07CH₂Cl₂) C, H, N.

5.3.3. *N*-[(3aS*,4S*,6aR*)-2-Benzyl-octahydrocyclopenta[c]pyrrol-4-yl]-2-cyclohexyl-2-phenylacetamide (40)

(29 mg, 30% yield): ¹H NMR (500 MHz, pyridine-*d*₅) δ ppm 8.06 (dd, *J* = 6.8, 23.5, 1H), 7.67 (d, *J* = 7.2, 1H), 7.46–7.39 (m, 3H), 7.40–7.29 (m, 4H), 7.29–7.22 (m, 1H), 4.45–4.37 (m, 0.5H), 4.35–4.27 (m, 0.5H), 3.54 (d, *J* = 12.7, 0.5H), 3.42 (dd, *J* = 4.0, 12.8, 1H), 3.34–3.19 (m, 1.5H), 2.97–2.77 (m, 2.5H), 2.63 (d, *J* = 7.2, 0.5H), 2.46–2.27 (m, 3H), 2.26–2.05 (m, 1.5H), 2.03–1.84 (m, 1.5H), 1.71 (dt, *J* = 7.0, 14.1, 0.5H), 1.65–1.36 (m, 8H), 1.33–1.22 (m, 0.5H), 1.20–0.98 (m, 2H); MS (ESI+) *m/z* 403(M+H)⁺; Anal. (C₂₇H₃₄N₂O) C, H, N.

5.3.4. *N*-[(3aR*,4R*,6aS*)-2-Benzyl-octahydrocyclopenta[c]pyrrol-4-yl]-2-cyclohexyl-2-phenylacetamide (41)

(41 mg, 41% yield): ¹H NMR (500 MHz, pyridine-*d*₅) δ ppm 8.10 (s, 1H), 7.67 (d, *J* = 7.2, 1H), 7.44 (dd, *J* = 5.7, 12.3, 3H), 7.40–7.35 (m, 3H), 7.33 (t, *J* = 7.4, 1H), 7.27 (dd, *J* = 7.6, 16.2, 1H), 4.43–4.37 (m, 0.5H), 4.36–4.29 (m, 0.5H), 3.56 (d, *J* = 12.6, 0.5H), 3.42 (t, *J* = 11.7, 1H), 3.26 (dd, *J* = 6.6, 11.7, 1H), 3.14 (d, *J* = 10.5, 0.5H), 2.80 (d, *J* = 8.3, 1H), 2.63 (d, *J* = 6.9, 0.5H), 2.24–2.13 (m, 1.5H), 2.02 (d, *J* = 12.5, 0.5H), 1.91 (d, *J* = 7.0, 1H), 1.74–1.59 (m, 2.5H), 1.58–1.34 (m, 4H), 1.33–1.19 (m, 1.5H), 1.18–0.99 (m, 3H), 0.87 (d, *J* = 14.3, 0.5H), 0.81–0.68 (m, 1H); MS (ESI+) *m/z* 417 (M+H)⁺; Anal. (C₂₈H₃₆N₂O) C, H, N.

5.3.5. *N*-[(3aS*,4S*,6aR*)-2-Benzyl-octahydrocyclopenta[c]pyrrol-4-yl]-1-phenylcyclopentanecarboxamide (42)

(40 mg, 42% yield): ¹H NMR (500 MHz, pyridine-*d*₅) δ ppm 7.52–7.28 (m, 9H), 7.25 (d, *J* = 7.7, 1H), 4.43–4.34 (m, 1H), 3.56 (d, *J* = 12.9, 1H), 3.17 (d, *J* = 12.9, 1H), 2.83–2.67 (m, 2H), 2.59–2.50 (m, 1H), 2.50–2.44 (m, 1H), 2.35–2.29 (m, 2H), 2.04–1.87 (m, 4H), 1.84–1.54 (m, 6H), 1.43–1.26 (m, 1H), 1.04–0.94 (m, 1H); MS (ESI+) *m/z* 389 (M+H)⁺; Anal. (C₂₆H₃₂N₂O) C, H, N.

5.3.6. *N*-[(3aS*,4S*,6aR*)-2-Benzyl-octahydrocyclopenta[c]pyrrol-4-yl]-1-phenylcyclohexanecarboxamide (43)

(34 mg, 35% yield): ¹H NMR (500 MHz, pyridine-*d*₅) δ ppm 7.57–7.54 (m, 2H), 7.45 (t, *J* = 7.3, 2H), 7.37 (dd, *J* = 7.6, 15.3, 5H), 7.29 (d, *J* = 6.9, 1H), 7.25 (t, *J* = 7.3, 1H), 4.41 (m, 1H), 3.59 (d, *J* = 12.9, 1H), 3.18 (d, *J* = 12.9, 1H), 2.52 (dd, *J* = 8.9, 17.6, 4H), 2.34 (dd, *J* = 8.5, 15.2, 2H), 2.01–1.92 (m, 2H), 1.91–1.80 (m, 2H), 1.79–1.68 (m, 3H), 1.61 (d, *J* = 25.2, 4H), 1.43–1.33 (m, 1H), 1.27 (d, *J* = 8.7, 1H), 1.04–0.93 (m, 1H); MS (ESI+) *m/z* 403 (M+H)⁺; Anal. (C₂₇H₃₄N₂O) C, H, N.

5.3.7. 2-ethyl-*N*-[(3aS*,4S*,6aR*)-2-[3-(trifluoromethyl)benzyl]octahydrocyclopenta[c]pyrrol-4-yl]butanamide (7)

(158 mg, 98% yield): ¹H NMR (500 MHz, pyridine-*d*₅) δ ppm 7.90 (d, *J* = 6.7, 1H), 7.71 (s, 1H), 7.61 (d, *J* = 7.7, 1H), 7.54 (d, *J* = 7.7, 1H), 7.46 (t, *J* = 7.7, 1H), 4.51–4.43 (m, 1H), 3.49 (s, 2H), 2.83 (ddd, *J* = 2.9, 7.8, 16.8, 1H), 2.75 (dd, *J* = 2.9, 9.5, 1H), 2.52–2.43 (m, 1H), 2.37 (dd, *J* = 2.9, 9.1, 1H), 2.35–2.30 (m, 1H), 2.25 (dd, *J* = 7.6, 9.4, 1H), 2.01 (tt, *J* = 4.8, 9.5, 1H), 1.89 (dt, *J* = 7.3, 11.6, 1H), 1.77 (ddt, *J* = 7.5, 9.3, 15.2, 2H), 1.70–1.60 (m, 2H), 1.51–1.37 (m, 2H), 1.34–1.26 (m, 1H), 0.95 (t, *J* = 7.4, 3H), 0.83 (t, *J* = 7.4, 3H); MS (ESI+) *m/z* 383(M+H)⁺; Anal. (C₂₁H₂₉F₃N₂O·0.06CH₂Cl₂) C, H, N.

5.3.8. 2-Propyl-*N*-[(3aS*,4S*,6aR*)-2-[3-(trifluoromethyl)benzyl]octahydrocyclopenta[c]pyrrol-4-yl]pentanamide (8)

(130 mg, 75% yield): ¹H NMR (500 MHz, pyridine-*d*₅) δ ppm 7.94 (d, *J* = 6.9, 1H), 7.72 (s, 1H), 7.62 (d, *J* = 7.7, 1H), 7.56 (d, *J* = 7.7, 1H), 7.47 (t, *J* = 7.7, 1H), 4.48 (dt, *J* = 7.3, 14.6, 1H), 3.52 (d, *J* = 13.0, 1H), 3.48 (d, *J* = 13.0, 1H), 2.84 (ddd, *J* = 3.0, 7.7, 16.7, 1H), 2.74 (dd, *J* = 3.1, 9.5, 1H), 2.52–2.45 (m, 1H), 2.38–2.34 (m, 2H), 2.27 (dd, *J* = 7.6, 9.5, 1H), 2.22 (td, *J* = 4.6, 9.5,

1H), 1.90 (dt, *J* = 7.3, 11.5, 1H), 1.84–1.75 (m, 2H), 1.73–1.61 (m, 2H), 1.48–1.27 (m, 6H), 1.20–1.08 (m, 1H), 0.88 (t, *J* = 7.0, 3H), 0.83 (t, *J* = 7.1, 3H); MS (ESI+) *m/z* 411(M+H)⁺; Anal. (C₂₃H₃₃F₃N₂O) C, H, N.

5.3.9. 2,2-Dicyclohexyl-*N*-[(3aS*,4S*,6aR*)-2-[3-(trifluoromethyl)benzyl]octahydrocyclopenta[c]pyrrol-4-yl]acetamide (9)

(176 mg, 97% yield): ¹H NMR (400 MHz, pyridine-*d*₅) δ ppm 7.73 (s, 1H), 7.65 (d, *J* = 7.6, 1H), 7.57–7.44 (m, 3H), 4.46 (dt, *J* = 6.4, 12.6, 1H), 3.55 (d, *J* = 12.9, 1H), 3.47 (d, *J* = 12.8, 1H), 2.75 (d, *J* = 8.1, 2H), 2.53–2.39 (m, 2H), 2.32 (t, *J* = 8.2, 1H), 2.21 (t, *J* = 8.3, 1H), 1.97–1.53 (m, 15H), 1.50–1.04 (m, 11H), 0.98 (dd, *J* = 11.3, 23.1, 1H); MS (ESI+) *m/z* 491(M+H)⁺; Anal. (C₂₉H₄₁F₃N₂O) C, H, N.

5.3.10. *N*-[(3aS*,4S*,6aR*)-2-[3-(Trifluoromethyl)benzyl]octahydrocyclopenta[c]pyrrol-4-yl]cyclopentanecarboxamide (10)

(120 mg, 75% yield): ¹H NMR (500 MHz, pyridine-*d*₅) δ ppm 7.82 (d, *J* = 6.9, 1H), 7.71 (s, 1H), 7.61 (d, *J* = 7.7, 1H), 7.55 (d, *J* = 7.7, 1H), 7.46 (t, *J* = 7.7, 1H), 4.48–4.41 (m, 1H), 4.07 (q, *J* = 7.1, 1H), 2.82 (ddd, *J* = 2.9, 7.8, 16.7, 1H), 2.72 (dd, *J* = 2.9, 9.5, 1H), 2.66 (p, *J* = 7.9, 1H), 2.50–2.42 (m, 1H), 2.37 (dd, *J* = 2.9, 9.0, 1H), 2.34–2.29 (m, 1H), 2.21 (dd, *J* = 7.5, 9.4, 1H), 2.03 (dt, *J* = 7.0, 15.3, 1H), 1.86 (dddd, *J* = 7.4, 12.3, 20.5, 23.4, 3H), 1.75–1.60 (m, 5H), 1.53–1.41 (m, 2H), 1.30 (td, *J* = 4.7, 11.1, 1H), 1.11 (t, *J* = 7.1, 1H); MS (ESI+) *m/z* 381(M+H)⁺; Anal. (C₂₁H₂₇F₃N₂O) C, H, N.

5.3.11. *N*-[(3aS*,4S*,6aR*)-2-[3-(Trifluoromethyl)benzyl]octahydrocyclopenta[c]pyrrol-4-yl]cyclohexanecarboxamide (11)

(127 mg, 76% yield): ¹H NMR (500 MHz, pyridine-*d*₅) δ ppm 7.74 (d, *J* = 6.1, 1H), 7.71 (s, 1H), 7.62 (d, *J* = 7.7, 1H), 7.57 (d, *J* = 9.2, 1H), 7.47 (t, *J* = 7.7, 1H), 4.48–4.41 (m, 1H), 3.53 (d, *J* = 13.2, 1H), 3.47 (d, *J* = 13.2, 1H), 2.84 (ddd, *J* = 2.8, 7.9, 10.3, 1H), 2.75 (dd, *J* = 2.8, 9.5, 1H), 2.51–2.43 (m, 1H), 2.37 (dd, *J* = 2.8, 9.1, 1H), 2.34–2.29 (m, 1H), 2.27–2.19 (m, 2H), 1.94–1.83 (m, 2H), 1.80 (d, *J* = 12.9, 1H), 1.73–1.60 (m, 6H), 1.57–1.51 (m, 1H), 1.35–1.27 (m, 1H), 1.22–1.10 (m, 3H); MS (ESI+) *m/z* 395(M+H)⁺; Anal. (C₂₂H₂₉F₃N₂O) C, H, N.

5.3.12. *N*-[(3aS*,4S*,6aR*)-2-[3-(Trifluoromethyl)benzyl]octahydrocyclopenta[c]pyrrol-4-yl]cycloheptanecarboxamide (12)

(104 mg, 60% yield): ¹H NMR (500 MHz, pyridine-*d*₅) δ ppm 7.79 (d, *J* = 6.9, 1H), 7.71 (s, 1H), 7.62 (d, *J* = 7.7, 1H), 7.56 (s, 1H), 7.47 (t, *J* = 7.7, 1H), 4.48–4.40 (m, 1H), 3.54 (d, *J* = 13.2, 1H), 3.46 (d, *J* = 13.2, 1H), 2.86 (ddd, *J* = 3.0, 7.8, 16.6, 1H), 2.76 (dd, *J* = 3.0, 9.5, 1H), 2.51–2.39 (m, 2H), 2.37–2.30 (m, 2H), 2.26 (dd, *J* = 7.5, 9.4, 1H), 2.00–1.80 (m, 5H), 1.75–1.60 (m, 4H), 1.49–1.41 (m, 4H), 1.33 (ddt, *J* = 7.2, 8.9, 12.1, 3H); MS (ESI+) *m/z* 409(M+H)⁺; Anal. (C₂₃H₃₁F₃N₂O) C, H, N.

5.3.13. 2,2-Diphenyl-*N*-[(3aS*,4S*,6aR*)-2-[3-(trifluoromethyl)benzyl]octahydrocyclopenta[c]pyrrol-4-yl]acetamide (13)

(100 mg, 39% yield): ¹H NMR (500 MHz, pyridine-*d*₅) δ ppm 8.50 (s, 1H), 7.71 (d, *J* = 7.5, 2H), 7.63 (d, *J* = 7.2, 2H), 7.45 (d, *J* = 7.4, 2H), 7.39–7.28 (m, 5H), 7.25 (dd, *J* = 5.8, 8.9, 3H), 4.51–4.42 (m, 1H), 3.44 (d, *J* = 13.3, 1H), 3.25 (d, *J* = 13.3, 1H), 2.85 (qd, *J* = 3.2, 7.9, 1H), 2.59 (dd, *J* = 3.4, 9.5, 1H), 2.47–2.37 (m, 1H), 2.26 (t, *J* = 8.3, 1H), 2.21–2.13 (m, 2H), 1.85–1.76 (m, 1H), 1.67–1.52 (m, 3H), 1.27–1.18 (m, 1H); MS (ESI+) *m/z* 479(M+H)⁺; Anal. (C₂₉H₂₉F₃N₂O·1.4HCl) C, H, N.

5.3.14. 2,2-Bis(4-fluorophenyl)-*N*-[(3aS*,4S*,6aR*)-2-[3-(trifluoromethyl)benzyl]octahydrocyclopenta[c]pyrrol-4-yl]acetamide (14)

(51 mg, 22% yield): ¹H NMR (500 MHz, pyridine-*d*₅) δ ppm 8.68 (d, *J* = 7.0, 1H), 7.64 (s, 1H), 7.60 (t, *J* = 6.4, 1H), 7.57–7.54 (m, 2H), 7.52–7.43 (m, 4H), 7.17–7.07 (m, 4H), 4.48–4.41 (m, 1H), 3.46 (d,

$J = 13.3$, 1H), 3.30 (d, $J = 13.3$, 1H), 2.90 (qd, $J = 3.5$, 8.0, 1H), 2.59 (dd, $J = 3.5$, 9.5, 1H), 2.50–2.42 (m, 1H), 2.32 (t, $J = 8.3$, 1H), 2.25–2.19 (m, 3H), 1.87–1.77 (m, 1H), 1.66 (td, $J = 5.7$, 11.4, 1H), 1.62–1.54 (m, 1H), 1.29–1.20 (m, 1H); MS (ESI+) m/z 515(M+H)⁺; Anal. (C₂₉H₂₇F₅N₂O·1HCl) C, H, N.

5.3.15. 3-Methyl-2-phenyl-N-((3aS*,4S*,6aR*)-2-[3-(trifluoromethyl)benzyl]octahydrocyclopenta[c]pyrrol-4-yl)butanamide (15)

(745 mg, 95% yield, white solid): ¹H NMR (500 MHz, pyridine-*d*₅) δ ppm 8.23 (d, $J = 6.9$, 0.5H), 8.13 (d, $J = 7.1$, 0.5H), 7.73 (s, 0.5H), 7.67 (s, 0.5H), 7.63 (dd, $J = 6.7$, 8.0, 2H), 7.56–7.53 (m, 1H), 7.50 (t, $J = 8.5$, 2H), 7.38–7.22 (m, 3H), 4.45–4.38 (m, 0.5H), 4.33–4.26 (m, 0.5H), 3.50 (s, 1H), 3.44 (d, $J = 13.4$, 0.5H), 3.21 (d, $J = 13.4$, 0.5H), 3.17 (d, $J = 10.5$, 0.5H), 3.10 (d, $J = 10.5$, 0.5H), 2.91 (qd, $J = 3.4$, 7.9, 0.5H), 2.79 (dd, $J = 3.4$, 9.5, 0.5H), 2.74–2.56 (m, 1.5H), 2.47–2.31 (m, 2.5H), 2.27 (dd, $J = 3.1$, 8.9, 0.5H), 2.21 (d, $J = 2.7$, 0.5H), 1.98–1.93 (m, 0.5H), 1.89–1.79 (m, 0.5H), 1.74–1.56 (m, 1.5H), 1.53–1.46 (m, 0.5H), 1.46–1.39 (m, 0.5H), 1.30–1.23 (m, 1H), 1.19 (d, $J = 6.5$, 1.5H), 1.17–1.11 (m, 0.5H), 1.08 (d, $J = 6.5$, 1.5H), 0.72 (dd, $J = 6.7$, 9.6, 3H); MS (ESI+) m/z 445 (M+H)⁺; Anal. (C₂₆H₃₁F₃N₂O) C, H, N.

5.3.16. N-[(3aS,4S,6aR)-2-Benzyl octahydrocyclopenta[c]pyrrol-4-yl]-2,2-dicyclohexylacetamide (23)

(468 mg, 77% yield): ¹H NMR (500 MHz, pyridine-*d*₅) δ ppm 7.44–7.38 (m, 4H), 7.37–7.32 (m, 1H), 4.49–4.38 (m, 1H), 3.57 (d, $J = 12.6$, 1H), 3.37 (d, $J = 12.5$, 1H), 2.77 (dd, $J = 1.7$, 9.6, 1H), 2.68 (td, $J = 2.0$, 9.3, 1H), 2.51 (dd, $J = 1.9$, 9.0, 1H), 2.45 (dd, $J = 7.1$, 15.9, 1H), 2.30–2.25 (m, 1H), 2.11 (dd, $J = 7.1$, 9.6, 1H), 1.98–1.83 (m, 3H), 1.83–1.58 (m, 12H), 1.57–1.51 (m, 1H), 1.48 (d, $J = 13.0$, 1H), 1.44–1.37 (m, 1H), 1.36–1.09 (m, 9H), 1.04–0.94 (m, 1H); MS (ESI+) m/z 423(M+H)⁺; Anal. (C₂₈H₄₂N₂O·0.5H₂O) C, H, N.

5.3.17. 2,2-Dicyclohexyl-N-((3aR,4R,6aS)-2-[3-(trifluoromethyl)benzyl]octahydrocyclopenta[c]pyrrol-4-yl)acetamide (37)

(0.780 g, 45% yield): [α]_D²⁰ +68.9° (c 1.02, CH₃OH) ¹H NMR (500 MHz, pyridine-*d*₅) δ ppm 7.73 (s, 1H), 7.66 (d, $J = 7.7$, 1H), 7.55 (d, $J = 7.3$, 2H), 7.50 (t, $J = 7.7$, 1H), 4.50–4.43 (m, 1H), 3.54 (d, $J = 12.9$, 1H), 3.46 (d, $J = 12.9$, 1H), 2.74 (td, $J = 2.6$, 10.5, 2H), 2.51–2.42 (m, 2H), 2.31 (t, $J = 8.3$, 1H), 2.20 (dd, $J = 7.8$, 9.8, 1H), 1.94–1.54 (m, 15H), 1.46 (d, $J = 13.0$, 1H), 1.40 (d, $J = 14.4$, 1H), 1.35–1.07 (m, 9H), 0.98 (qd, $J = 3.0$, 12.3, 1H); MS (ESI+) m/z 491(M+H)⁺; Anal. (C₂₉H₄₁F₃N₂O·1HCl·2.3H₂O) C, H, N.

5.4. Single crystal X-ray diffraction studies

A single crystal of compound **20** was mounted on a glass fiber. Intensity data were collected on a Bruker SMART system equipped with an APEX CCD camera. Data were collected at 173 K with graphite-monochromated MoK α radiation ($\lambda = 0.71073$ Å). Data were collected in four sets using omega-phi scans with omega steps of 0.3° and phi steps of 90°. A total of 2350 frames were collected with 20 s frame exposures. Data were processed using SaintPlus.²⁵ Corrections for Lorentz-polarization effects were applied. Absorption was negligible. All structures were solved using direct methods that yielded the non-hydrogen atoms. All presented hydrogen atoms were located in Fourier-difference electron density maps. All non-hydrogen atoms were refined anisotropically. Hydrogen atoms associated with carbon atoms were refined in geometrically constrained riding positions. The hydrogen atom associated with the sulfonamide nitrogen atom was included in the located positions. Refinement was achieved with the use of SHELX-97.²⁶

5.5. Biological assays

5.5.1. N-type FLIPR Assay

The N-type FLIPR assay was performed as described previously.^{17,24} Briefly, IMR32 human neuroblastoma cells were plated at a density of 120,000 cells per well and incubated for 48 h at 37 °C with 5% CO₂. Cells were incubated with 100 μ l of diluted Calcium 4 dye prepared in HBSS containing 1 mM HEPES, pH 7.4 for 1.5 h at room temperature. Antagonists (50 μ l) were pre-incubated during dye loading for 1 h prior to the addition of depolarizing buffer (50 μ l, HBSS) containing 80 mM KCl in the presence of 5 mM CaCl₂. Experiments were completed in the presence of 2 μ M nifedipine to block endogenous L-type calcium channels. Data are plotted as the percent of control response in the absence of antagonist and IC₅₀ values were determined following nonlinear regression analysis.

5.5.2. L-type FLIPR assay

ND7/23 cells were maintained in Dulbecco's Modified Eagle's Medium (DMEM) containing 10% (v/v) heat-inactivated FBS. Following dissociation with enzyme-free PBS-based buffer, cells were resuspended in growth media and seeded at a density of 5.0×10^4 cells per well in 96-well poly-D-Lysine coated plates. Cells were incubated for 24 h at 37 °C in a humidified incubator with 5% CO₂ prior to use in the calcium mobilization assay. Calcium dye (10 \times) (Molecular Devices) was diluted 1:10 with HBSS containing 20 mM HEPES, pH 7.4 (buffer A). The growth media was removed using gently aspiration and the cells were then incubated with 100 μ l of diluted calcium dye for 1.5 h at room temperature. The compounds (50 μ l) prepared in buffer A were incubated with the cells for 3 min at room temperature prior to activation of L-type Ca²⁺ channels by addition of a high concentration of KCl and CaCl₂, 50 mM and 2.5 mM, respectively in HBSS in 50 μ l. Data are plotted as the percent of control response in the absence of antagonist and IC₅₀ values were determined using nonlinear regression analysis.

5.5.3. Whole cell patch clamp studies

The N-type cell line stably co-expressing rat recombinant Cav2.2 exons [Δ 18a, Δ 24a, 31a, 37b], Cav β 3, and α 2 δ 1 subunits was obtained from Dr. Diane Lipscombe (Brown University). Cells were maintained at 37 °C and 5% CO₂ in growth media containing Dulbecco's modified Eagle's medium supplemented with 10% fetal bovine serum, 1% GlutaMAX, 100 IU/mL penicillin, 100 mg/mL streptomycin, 10 μ g/mL blasticidin, 50 μ g/mL hygromycin B, and 50 μ g/mL zeocin. All cell culture reagents were purchased from Invitrogen (Carlsbad, CA). Assessment of the activity of compound **25** at N-type calcium channels was performed using whole cell patch clamp analysis as described previously.¹⁷ Briefly, on the day of the experiment, cells plated in a T25 cell culture flasks and grown to 60–80% confluency were rinsed once in DPBS and dissociated with 5 ml Detachin (Genlantis, San Diego, CA) at 37 °C for 4–5 min. Dissociated cells were then centrifuged at 1200 rpm for 4 min at room temperature, the supernatant was removed, and the pellet was re-suspended in growth media. Membrane currents were recorded from the stable N-type HEK293 cell line using the whole-cell patch clamp technique. Fire-polished borosilicate glass electrodes had resistances from 1–3 M Ω when filled with internal solution which contained (in mM): 101 CsCl, 24 CsF, 1.8 NaCl, 7.4 EGTA, 9 HEPES, 4 Mg₂ATP, 14 Creatine phosphate, and 0.3 GTP, pH 7.4 adjusted with CsOH and an osmolality of approximately 290 mOsm. Cell were superfused with extracellular solution which contained (in mM): 87.5 CsCl, 40 (TEA)-Cl, 10 HEPES, 10 glucose, 5 BaCl₂, and 1 MgCl₂, pH 7.2, 310 mOsm. To evaluate compound potency, cells were first voltage clamped at –115 mV and stepped to 0 mV once every 15 s to determine the cells maximal current. Cells

were then voltage-clamped at -80 to -95 mV and stepped to 0 mV once every 5 s to induce a degree of channel inactivation. After a stable control baseline current was obtained, compound was added in escalating concentrations of 1 to 3 concentrations per cell and percent control values were determined after steady state inhibition was achieved at each concentration. GraphPad Prism (GraphPad Software, San Diego, CA) was used for data plotting and data fitting.

5.5.4. Rat aorta ring tissue relaxation assay

The activity of compound **25** at native L-type calcium channels was assessed using rat aorta ring tissue as described previously.¹⁷ Briefly, male Sprague–Dawley rats (200–350 g; Charles River Laboratories, Wilmington, MA) were euthanized with CO_2 and decapitated. The entire thoracic aorta was removed and immediately placed into Krebs Ringer bicarbonate solution and equilibrated with $5\% \text{CO}_2$; $95\% \text{O}_2$. Propranolol (Sigma–Aldrich, 0.004 mM) was included in all of the assays to block β adrenoreceptors. The aorta was cut into 3 – 4 mm rings and mounted in 10 ml isolated tissue baths at 37°C . The aorta from each rat supplied 8 tissue rings with one end of the aorta fixed to a stationary glass rod and the other to a Grass FT03 transducer at a basal preload of 1.0 g. The aorta was primed once with 80 mM KCl, rinsed and allowed to return to basal tension and primed again with 10 μM phenylephrine (PE). After an additional 30 min equilibration period tension was established using 80 mM KCl solution. A relaxation concentration response curve was generated for each tissue. Data collection was by Power-Lab/800 data acquisition system (Castle Hill, Australia). The amount of compound **25** necessary to cause a 50% reversal (ED_{50}) of 80 mM KCl evoked contraction was calculated by nonlinear regression analysis using the Levenberg–Marquardt curve fitting algorithm in GraphPad Prism.

5.6. In vivo characterization

5.6.1. Animals

Male Sprague–Dawley rats (200–350 g, Charles River Laboratories, Wilmington, MA, USA) were used for behavioral assessment. All procedures were performed in an Association for Assessment and Accreditation of Laboratory Animals Care (AAALAC) approved facility and approved by the Institutional Animals Care and Use Committee (IACUC) at Abbott Laboratories. Compound **25** was administered by intraperitoneal injection (ip), prepared in 10% dimethylsulfoxide (DMSO)/polyethylene glycol 400 (PEG) (Sigma–Aldrich, St. Louis, MO, USA) in a volume of 2.0 ml/kg. One way analysis of variance (one-way ANOVA) was performed for all data analysis. Post hoc analyses were performed using Bonferroni: compared selective pairs of columns for multiple comparisons (GraphPad Prism, GraphPad Software, Inc., USA).

5.6.2. Carrageenan thermal hypersensitivity

Acute thermal hypersensitivity was induced by injecting 100 μl of a 1% solution of λ -carrageenan (Sigma Chemical Co., St. Louis, MO) in physiological saline into the plantar surface of the right hind paw. Thermal hypersensitivity was determined 2 h following carrageenan injection, using a commercially available thermal paw stimulator (UARDG, University of California, San Diego, CA) as described by Hargreaves et al.²⁷ Rats were placed into individual plastic cubicles mounted on a glass surface maintained at 30°C , where a thermal stimulus was then applied to the plantar surface of each hind paw. The stimulus current was maintained at 4.50 ± 0.05 amp, and the maximum time of exposure was set at 20.48 s to limit possible tissue damage. The elapsed time until a brisk withdrawal of the hind paw from the thermal stimulus was recorded automatically using photodiode motion sensors. The right and left hind paw of each rat was tested in 3 sequential trials at approximately 5 min intervals. Carrageenan-induced thermal

hypersensitivity of paw withdrawal latency (PWL) was calculated as the mean of the two shortest latencies. Compound **25** (3 , 10 , 30 mg/kg, ip, $n = 6$) was administered 30 min prior to the assessment of thermal hypersensitivity.

5.6.3. Monoiodoacetic acid (MIA) induced osteoarthritis pain

Under light (2 – 4%) isoflurane (Baxter, IL, USA) anesthesia, MIA (3 mg/rat in 50 μl sterile isotonic saline) was intra-articularly injected into right knee joint cavity of the hind leg using a 26G needle. Measurements of peak hind limb grip force were conducted at least 21 days following MIA-injection as described previously.²⁸ Each rat was sequentially tested twice at approximately 2 -minute intervals to obtain a maximum compressive grip force (CF_{max}) exerting on the hindlimb strain gauge, in a commercially available grip force measurement system (Columbus Instruments, Columbus, OH, USA). The impact of body weight on grip force was calculated using the formula: $\text{g} (\text{CF}_{\text{max}})/\text{kg}$ (body weight). Compound **25** (3 , 10 , and 30 mg/kg, ip) was administered 30 min prior to grip force assessment. The vehicle control group was taken as 0% , whereas an age-matched naïve group was designated as 100% (normal).

5.6.4. Formalin induced persistent pain

The formalin assay was performed following the procedure originally described by Dubuisson and Dennis²⁹; 50 μl of a 5% formalin solution was injected subcutaneously (s.c.) into the dorsal aspect of the right hind paw and the rats were then individually placed into clear observation cages. Rats were observed for a period of 20 min (30 – 50 min following formalin injection).³⁰ The number of flinching behaviors of the injected paw was recorded using a sampling technique in which each animal was observed for one 60 -second period during each 5 -minute interval; thus twelve 60 -second observation periods were recorded. Compound **25** (3 , 10 , 30 mg/kg, ip, $n = 6$) was administered 30 min prior to formalin injection.

5.6.5. Rotarod

Rotarod performance was measured using an accelerating rotarod apparatus (Omnitech Electronics, Inc. Columbus, OH, USA) as described previously.¹⁷ Each rat was given three training sessions by being placed on a 9 cm diameter rod that increased in speed from 0 to 20 rpm over a 60 s period. The time required for the rat to fall from the rod was recorded, with a cut off score of 60 s. Compound **25** (3 , 10 and 30 mg/kg, ip, $n = 6$ per group) was then administered, and the animals were placed back on the rotarod apparatus for 3 consecutive testing trials 30 min following the compound administration.

5.6.6. Anesthetized rat cardiovascular studies

The effects of Compound **25** on hemodynamic and cardiovascular function in the anesthetized rat were performed as described previously.³¹

Acknowledgements

The authors would like to thank the HT-ADME group for micro-somal stability and solubility data, the structural chemistry group for 1H NMR and MS on all compounds and Paul Wiedeman for careful reading of the manuscript.

References and notes

1. Kisilevsky, A. E.; Zamponi, G. W. *Handb. Exp. Pharmacol.* **2008**, *184*, 45.
2. Cao, Y. *Pain* **2006**, *126*, 5.
3. Ertel, E. A.; Campbell, K. P.; Harpold, M. M.; Hofmann, F.; Mori, Y.; Perez-Reyes, E.; Schwartz, A.; Snutch, T. P.; Tanabe, T.; Birnbaumer, L.; Tsien, R. W.; Catterall, W. A. *Neuron* **2000**, *25*, 533.
4. Barrett, T. D.; Triggie, D. J.; Walker, M. J. A.; Maurice, D. H. *Mol. Interv.* **2005**, *5*, 84.

5. McGivern, J. G. *Drug Discovery Today* **2006**, *11*, 245.
6. Yamamoto, T.; Takahara, A. *Curr. Top. Med. Chem.* **2009**, *9*, 377.
7. Schmidtke, A.; Lotsch, J.; Freynhagen, R.; Geisslinger, G. *Lancet* **2010**, 375, 1569.
8. Rauck, R. L.; Wallace, M. S.; Leong, M. S.; Minehart, M.; Webster, L. R.; Charapata, S. G.; Abraham, J. E.; Buffinton, D. E.; Ellis, D.; Kartzinell, R. J. *Pain Symptom Manage* **2006**, *31*, 393.
9. Pajouhesh, H.; Feng, Z.-P.; Ding, Y.; Zhang, L.; Pajouhesh, H.; Morrison, J.-L.; Belardetti, F.; Tringham, E.; Simonson, E.; Vanderah, T. W.; Porreca, F.; Zamponi, G. W.; Mitscher, L. A.; Snutch, T. P. *Bioorg. Med. Chem. Lett.* **2010**, *20*, 1378.
10. Zamponi, G. W.; Feng, Z.-P.; Zhang, L.; Pajouhesh, H.; Ding, Y.; Belardetti, F.; Pajouhesh, H.; Dolphin, D.; Mitscher, L. A.; Snutch, T. P. *Bioorg. Med. Chem. Lett.* **2009**, *19*, 6467.
11. Yamamoto, T.; Niwa, S.; Ohno, S.; Tokumasu, M.; Masuzawa, Y.; Nakanishi, C.; Nakajo, A.; Onishi, T.; Koganei, H.; Fujita, S.; Takeda, T.; Kito, M.; Ono, Y.; Saitou, Y.; Takahara, A.; Iwata, S.; Shoji, M. *Bioorg. Med. Chem. Lett.* **2008**, *18*, 4813.
12. Yamamoto, T.; Niwa, S.; Iwayama, S.; Koganei, H.; Fujita, S.; Takeda, T.; Kito, M.; Ono, Y.; Saitou, Y.; Takahara, A.; Iwata, S.; Yamamoto, H.; Shoji, M. *Bioorg. Med. Chem.* **2006**, *14*, 5333.
13. Knutsen, L. J.; Hobbs, C. J.; Earnshaw, C. G.; Fiumana, A.; Gilbert, J.; Mellor, S. L.; Radford, F.; Smith, N. J.; Birch, P. J.; Ward, S. D.; Russell Burley, J.; James, I. F. *Bioorg. Med. Chem. Lett.* **2007**, *17*, 662.
14. Hu, L.-Y.; Ryder, T. R.; Rafferty, M. F.; Cody, W. L.; Lotarski, S. M.; Miljanich, G. P.; Millerman, E.; Rock, D. M.; Song, Y.; Stoehr, S. J.; Taylor, C. P.; Weber, M. L.; Szoke, B. G.; Vartanian, M. G. *Bioorg. Med. Chem. Lett.* **1999**, *9*, 907.
15. Hu, L.-Y.; Ryder, T. R.; Nikam, S. S.; Millerman, E.; Szoke, B. G.; Rafferty, M. F. *Bioorg. Med. Chem. Lett.* **1999**, *9*, 1121.
16. Abbadie, C.; McManus, O. B.; Sun, S.-Y.; Bugianesi, R. M.; Dai, G.; Haedo, R. J.; Herrington, J. B.; Kaczorowski, G. J.; Smith, M. M.; Swensen, A. M.; Warren, V. A.; Williams, B.; Arneric, S. P.; Eduljee, C.; Snutch, T. P.; Tringham, E. W.; Jochnowitz, N.; Liang, A.; MacIntyre, D. E.; McGowan, E.; Mistry, S.; White, V. V.; Hoyt, S. B.; London, C.; Lyons, K. A.; Bunting, P. B.; Volksdorf, S.; Duffy, J. L. *J. Pharm. Exp. Ther.* **2010**, 334, 545.
17. Scott, V. E.; Vortherms, T. A.; Niforatos, W.; Swensen, A. M.; Neelands, T.; Milicic, I.; Banfor, P. N.; King, A.; Zhong, C.; Simler, G.; Zhan, C.; Bratcher, N.; Boyce-Rustay, J. M.; Zhu, C. Z.; Bhatia, P.; Doherty, G.; Mack, H.; Stewart, A. O.; Jarvis, M. F. *Biochem. Pharmacol.* **2012**, *83*, 406.
18. Doherty, G.; Bhatia, P.; Vortherms, T. A.; Marsh, K. C.; Wetter, J. M.; Mack, H.; Scott, V. E.; Jarvis, M. F.; Stewart, A. O. *Bioorg. Med. Chem. Lett.* **2012**, *22*, 1716.
19. Padwa, A.; Dent, W. J. *Org. Chem.* **1987**, *52*, 235.
20. Terao, Y.; Kotaki, H.; Imai, N.; Achiwa, K. *Chem. Pharm. Bull.* **1985**, *8*, 2762.
21. Santora, V. J.; Covell, J. A.; Hayashi, R.; Hoflana, B. J.; Ibarra, J. B.; Pulley, M. D.; Weinhouse, M. I.; Sengupta, D.; Duffield, J. J.; Semple, G.; Webb, R. R., et al. *Bioorg. Med. Chem. Lett.* **2008**, *18*, 1490.
22. Robak, M. T.; Herbage, M. A.; Ellman, J. A. *Chem. Rev.* **2010**, *110*, 3600.
23. Tanuwidjaja, J.; Peltier, H. M.; Ellman, J. A. *J. Org. Chem.* **2007**, *72*, 626.
24. Vortherms, T. A.; Swensen, A. M.; Niforatos, W.; Limberis, J. T.; Neelands, T. R.; Janis, R. S.; Thimmapaya, R.; Donnelly-Roberts, D. L.; Namovic, M. T.; Zhang, D.; Putman, C. B.; Martin, R. L.; Surowy, C. S.; Jarvis, M. F.; Scott, V. E. *Inflamm. Res.* **2011**, *60*, 683.
25. Bruker AXS Inc., SaintPlus, version 6.02, Madison Wisconsin, 1999.
26. Sheldrick, G. M. University of Göttingen, Germany, 1998.
27. Hargreaves, K.; Dubner, R.; Brown, F.; Flores, C.; Joris, J. *Pain* **1988**, *32*, 77.
28. Chandran, P.; Pai, M.; Blomme, E. A.; Hsieh, G. C.; Decker, M. W.; Honore, P. *Eur. J. Pharmacol.* **2009**, *613*, 39.
29. Dubuisson, D.; Dennis, S. G. *Pain* **1977**, *4*, 161.
30. Abbott, F. V.; Franklin, K. B.; Westbrook, R. F. *Pain* **1995**, *60*, 91.
31. Liu, G.; Zhao, H.; Liu, B.; Xin, Z.; Liu, M.; Serby, M. D.; Lubbers, N. L.; Widomski, D. L.; Polakowski, J. S.; Beno, D. W. A., et al. *Bioorg. Med. Chem. Lett.* **2007**, *17*, 495.